Table 3. Summary of the AlphaScreen Method and the Enzyme-Labeled Antigen Method in 10 Patients with Radicular Cyst

Case	1		2		3		4		5		6		7		8		9		10	
Age/sex	49M		42M		52M		50M		43M		38F		60F		47M		47F		28F	
Site	UM		UI		UI		UI		UI		LP		LM		LM		LM		UI	
Size (cm)	3.4		1.6		2.2		1.9		1.7		2.1		1.9		2.8		1.4		0.8	
Periodontitis	Moderate		Moderate		Mild		Moderate		Mild		None		None		Moderate		None		None	
Sample	T	S	T	S	T	S	T	S	T	S	T	S	T	S	T	S	T	S	T	S
AlphaScreen method																				
Ag53	1.4	1.7	NE	1.7	1.3	1.7	1.0	**2.1**	NE	1.4	0.9	1.3	NE	1.5	NE	1.4	0.9	1.4	0.8	1.2
Arg-pro	1.1	1.1	NE	1.3	1.1	1.2	0.7	1.3	NE	1.2	1.2	1.2	NE	1.2	NE	1.4	0.8	1.1	0.8	1.1
Arg-hgp	1.1	1.6	NE	1.3	**7.7**	1.6	1.2	**2.5**	NE	1.3	**7.4**	1.7	NE	1.4	NE	**4.2**	1.0	1.1	1.0	1.4
Lys-pro	1.2	1.4	NE	1.4	1.2	1.3	0.8	1.5	NE	1.2	1.0	1.2	NE	1.3	NE	**8.5**	1.5	1.2	1.0	1.2
Lys-hgp	1.2	1.8	NE	1.5	**3.4**	1.8	1.2	**2.5**	NE	1.3	**8.6**	1.7	NE	1.4	NE	**7.0**	1.0	1.3	1.7	1.6
SpaP	1.1	1.2	NE	1.3	1.1	1.3	0.7	1.4	NE	1.2	0.8	1.0	NE	1.3	NE	**4.2**	1.0	1.3	0.9	1.3
Enzyme-labeled antigen method																				
Ag53	–		–		–		NP		–		–		–		NP		–		–	
Arg-pro	–		–		–		NP		–		–		–		NP		–		–	
Arg-hgp	–		–		+		NP		–		+		–		NP		–		–	
Lys-pro	–		–		–		NP		–		–		–		NP		–		–	
Lys-hgp	–		–		–		NP		–		+		–		NP		–		–	
SpaP	–		–		–		NP		–		–		–		NP		–		–	

Site: UM, upper molar; UI, upper incisor; LP, lower premolar; LM, lower molar. Sample: T, tissue extract; S, serum. NE, not examined; NP, no plasma cells seen in frozen sections. AlphaScreen method: Data no less than 2.0 are regarded as positive, represented with bold figures. + indicates positive reaction with the enzyme-labeled antigen method.

extract from two of six cases examined (cases 3 and 6), but the specific antibodies were not elevated in the serum in these two cases. In contrast, specific antibodies were elevated in the serum in two cases (cases 4 and 8): In case 4, low serum titers against Ag53, Arg-hgp, and Lys-hgp were detected, and in case 8, high titers against Arg-hgp, Lys-hgp, Lys-pro, and SpaP were shown. In these two cases, however, plasma cells were scarcely observed in frozen sections of the surgically removed radicular cyst. When the degree of periodontitis was reviewed, these two cases complicated moderate-degree periodontitis. Although cases 1 and 2 also showed moderate-degree periodontitis, all the cases with mild-degree (n=2) or no (n=4) periodontitis were AlphaScreen negative.

On proteinase K–pretreated fixed frozen sections, plasma cells were infiltrated in a total of eight lesions of radicular cyst. Purified biotinylated proteins were used as probes, except for SpaP, for which crude (unpurified) solutions were applied. In cases 3 and 6, positive signals for Arg-hgp were detected by the enzyme-labeled antigen method. The cytoplasm of plasma cells, often clustered beneath the squamous epithelial lining, showed homogeneous positivity. Antibodies against Lys-hgp were also visualized in a small number of plasma cells in case 6. The AlphaScreen titration was very high (more than 7) in these positive cases. No signals were demonstrated in the other sections. Representative features in case 6 are illustrated in Figure 6.

The results of the double immunofluorescence study are illustrated in Figure 7. Inflammatory cells showing cytoplasmic signals positive for Arg-hgp in cases 3 and 6, as well as the cells positive for Lys-hgp in case 6, were labeled for CD138 mainly along the plasma membrane. The plasmacytic nature of the signal-positive cells was thus confirmed. Squamous epithelial cells were also CD138 positive.

When paraffin sections were reviewed, the histological features of cases 3 and 6 were indistinguishable from other cases. All but one (case 8) showed dense infiltration of plasma cells in the cyst wall. In case 4, plasma cells were plentiful in paraffin sections in contrast to frozen sections. Foamy cells were clustered in cases 5 and 10, and neutrophils were rich in case 7.

Absorption Test for Confirming the Specificity of Staining

The positive anti-Ag53 signals in plasma cells of rat lymph nodes were eliminated only with an excess amount of unlabeled Ag53 antigen. The positive signals of anti-Arg-hgp and anti-Lys-hgp reactivities were not eliminated with unlabeled Ag53, Arg-pro, and Lys-pro in both rat and

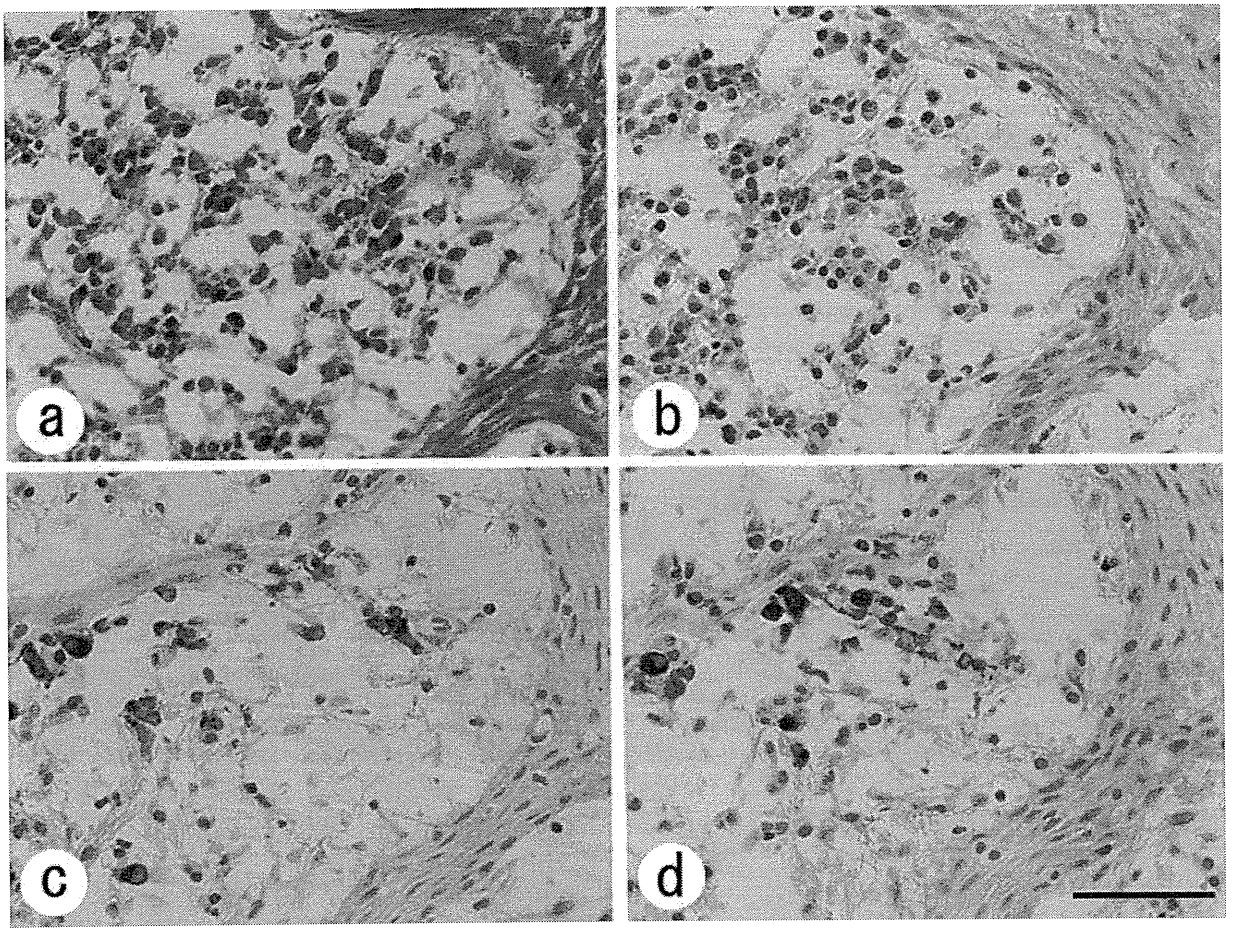

Figure 6. Visualization of plasma cells producing antibodies against *Porphyromonas gingivalis*–related proteins in proteinase K–pretreated frozen sections of radicular cyst (case 6) with the enzyme-labeled antigen method. Plasma cells are clustered beneath the squamous epithelial lining in the gingival cystic lesion (a: hematoxylin and eosin staining). Antibodies against Ag53 (b) are negative in the lesion, whereas antibodies against Arg-hgp (c) and Lys-hgp (d) are localized in the cytoplasm of plasma cells clustered just beneath the squamous epithelial lining. Bar indicates 50 μm.

human tissues. When biotinylated Arg-hgp or Lys-hgp was diluted with unlabeled Arg-hgp or Lys-hgp, a considerable percentage of the positive signals in plasma cells in rat and human tissues disappeared or became significantly weakened, indicating the production of antibodies against the common epitope between Arg-hgp and Lys-hgp (Fig. 8).

In the radicular cyst of case 6 and some lymph nodes of the rat (Fig. 8f), in addition to antibodies directed toward the common epitope, antibodies specific to either Arg-hgp or Lys-hgp were also demonstrated. In some areas of the case 6 lesion, clustered plasma cells were reactive with both biotinylated Arg-hgp and Lys-hgp, and the reactivity was considerably weakened after incubating with unlabeled Arg-hgp or Lys-hgp. In other areas, dispersed plasma cells were reactive with biotinylated Arg-hgp but not with biotinylated Lys-hgp, and the reactivity was weakened with unlabeled Arg-hgp but not with unlabeled Lys-hgp (Fig. 9). The plasma cells in the latter region were considered to produce antibodies against an Arg-hgp-specific epitope. Similarly, antibodies against Lys-hgp-specific epitopes were also recognized in plasma cells in case 6. In the case 3 lesion where anti-Arg-hgp signals were detected without signals against Lys-hgp, anti-Arg-hgp reactivity was abolished with Arg-hgp but not with Lys-hgp, again proving antibody production specific to the epitope unique in Arg-hgp.

Discussion

We documented herein the novel application of the AlphaScreen method and the enzyme-labeled antigen method for demonstrating antibody production against

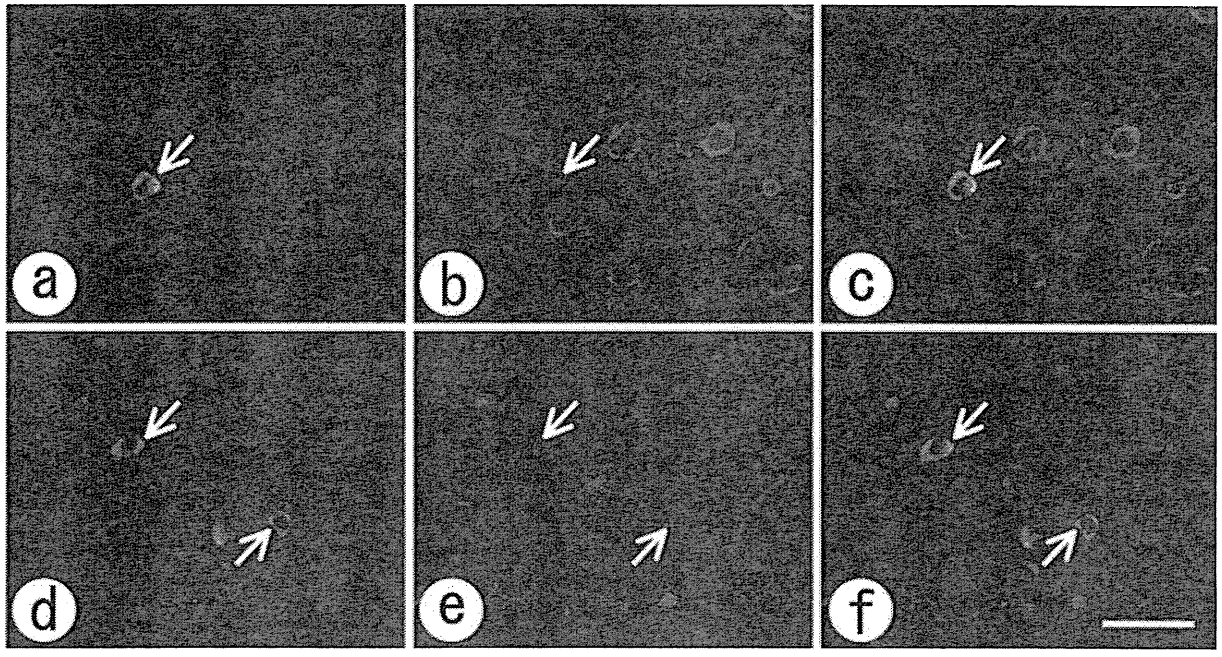

Figure 7. Double immunofluorescence analysis with biotinylated antigens and anti-CD138 monoclonal antibody in radicular cyst lesions (cases 3 and 6). The biotinylated antigens are stained green with Alexa Fluor 488 (a: Arg-hgp in case 3, d: Lys-hgp in case 6), whereas CD138 is immunolocalized in red with Alexa Fluor 568 (b, e). Panels c and f demonstrate merged pictures for both immunofluorescence. CD138 is expressed along the plasma membrane of the plasma cells positive for anti-Arg-hgp or anti-Lys-hgp. Arrows show the same plasma cells. Bar indicates 25 μm.

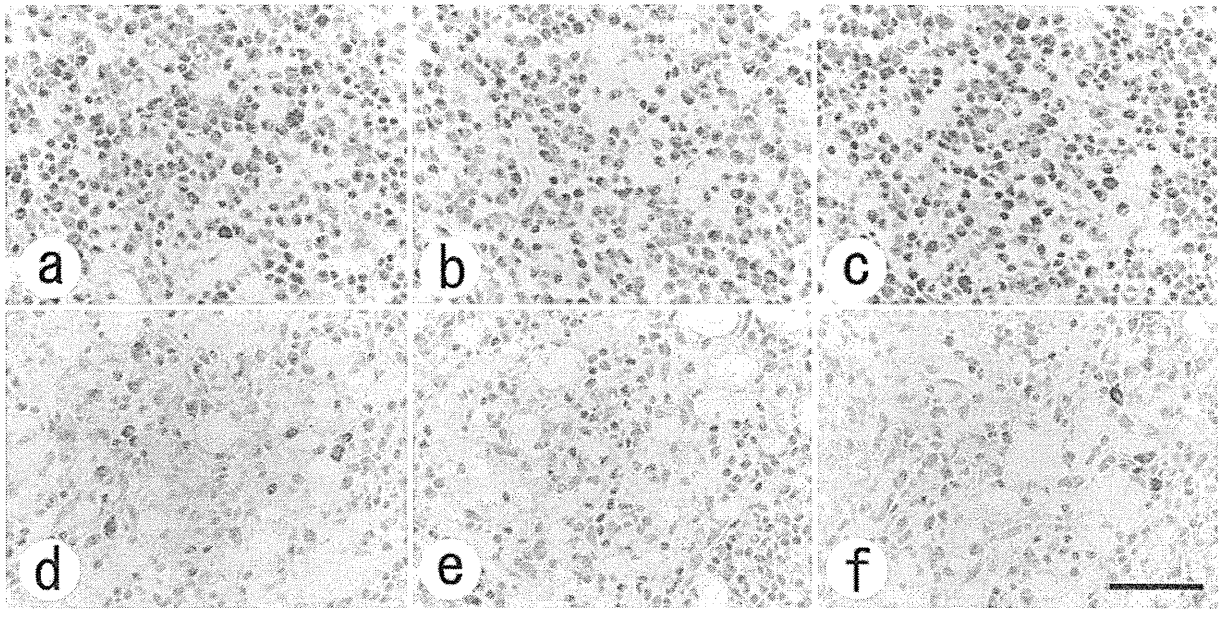

Figure 8. Absorption experiment (I) in rat axillary lymph node, showing the specificity of the enzyme-labeled antigen method (a–c: anti-Ag53 reactivity, d–f: anti-Arg-hgp reactivity). Anti-Ag53 reactivity (a) is mostly abolished with unlabeled Ag53 (b) but kept unchanged after addition of unlabeled Lys-hgp (c). Anti-Arg-hgp reactivity (d) is totally abolished with Arg-hgp (e). The addition of unlabeled Lys-hgp significantly weakens the signals in more than half of plasma cells, but some plasma cells remain strongly reactive (f). Bar indicates 50 μm.

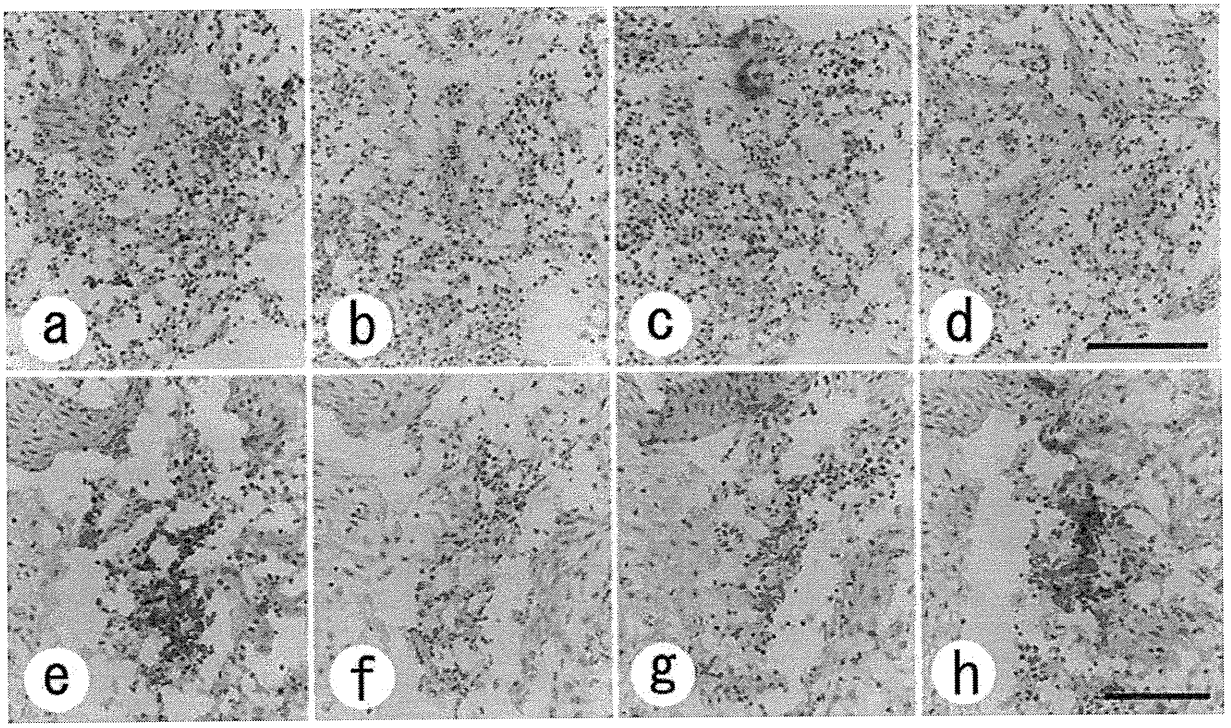

Figure 9. Absorption experiment (II) in radicular cyst in case 6, showing region specificity of the antibodies (a–d: area 1, e–h: area 2). Plasma cells with anti-Arg-hgp reactivity are scattered in area 1 (a) and densely clustered in area 2 (e). Addition of unlabeled Arg-hgp significantly abolishes the reactivity (b, f). Unlabeled Lys-hgp scarcely affects the reactivity in area 1 (c) but significantly weakens the reactivity in area 2 (g). Anti-Lys-hgp reactivity is not demonstrated in area 1 (d), whereas the same clusters are labeled with biotinylated Lys-hgp in area 2 (h). It is concluded that the plasma cells in area 1 produce antibodies against an epitope specific to Arg-hgp, whereas another epitope common to both Arg-hgp and Lys-hgp is recognized by the clonally clustered plasma cells in area 2. Bar indicates 100 μm.

P. gingivalis in the rat experimental system and in human radicular cyst lesions.

P. gingivalis is a black-pigmented, obligatory anaerobic gram-negative bacillus, often colonizing in the affected periodontal space in periodontitis or chronic gingivitis (Cutler et al. 1995; Slots and Ting 2000). Ag53 is a major outer membrane protein of *P. gingivalis* (Kurihara et al. 1991; Oyaizu et al. 2001), and positive immune response to Ag53 has been reported in patients with periodontitis (Kurihara et al. 1991; Schenkein 2006). *P. gingivalis* also expresses and secretes cysteine proteinases named gingipains (Chen et al. 2001; O'Brien-Simpson et al. 2001; Grenier and Tanabe 2010). Two major isoforms of gingipains are known: arginine-specific cysteine proteinase A (RgpA) and lysine-specific cysteine proteinase (Kgp). Each form consists of the proteinase domain (pro) and the hemagglutinin/adhesin domain (hgp). The hgps have been implicated as adhesins that actuate colonization of the epithelium lining the gingival sulcus. It has been reported that in cases of severe chronic periodontitis, the level of RgpA in periodontal pocket fluid correlated with the load of *P. gingivalis* (Guentsch et al. 2011). In the present study, we synthesized five *P. gingivalis* proteins such as Ag53, Arg-pro (pro in RgpA), Arg-hgp (hgp in RgpA), Lys-pro (pro in Kgp), and Lys-hgp (hgp in Kgp).

SpaP, a pathogenic major cell wall protein of *S. mutans* (Lee et al. 1988; Galaviz et al. 2002), was used as a negative control. The gram-positive cocci, residents in the human oral cavity, cause dental caries, and SpaP plays a major role in cell adherence to tooth surfaces and in sucrose-induced cell aggregation. DHFR, a folic acid–metabolizing enzyme reducing dihydrofolate to tetrahydrofolate, plays a housekeeping role in all proliferating cells (Feder et al. 1989). At the Cell-Free Science and Technology Research Center, Ehime University, *E. coli*–derived DHFR, synthesized with the cell-free protein synthesis system, has been used as a negative control (background level) in the AlphaScreen method (Sawasaki, Hasegawa, et al. 2002; Matsuoka et al. 2010).

The merits of the AlphaScreen method are as follows (Matsuoka et al. 2010). 1) In the reaction mixture, the antigens remain intact and thus functional. 2) Only small

aliquot of sample (0.025 μL serum per protein) is needed. 3) The antibody detection is highly efficient since no rinsing is needed, and multiple assays can be done simultaneously by using 384-well plates. 4) The sensitivity and specificity of detection are very high with low background.

Roughly speaking, the results obtained with both the AlphaScreen method and the enzyme-labeled antigen method corresponded. In the rat model, the enzyme-labeled antigen method was more sensitive than the AlphaScreen method, whereas in human cases, the AlphaScreen method seemed to be superior to the enzyme-labeled antigen method. The authors believe that with the aid of the AlphaScreen method, the validity and specificity of the new histochemical technique were proven in the present study. This might be the very first application of the enzyme-labeled antigen method to human tissues.

The following findings were particularly noteworthy from a technical and pathophysiological viewpoint.

1. Methodologically, the suitable technical sequences of the enzyme-labeled antigen method using paraformaldehyde-fixed frozen sections were comparable with those we recently reported in the rat experimental model (Mizutani et al. 2009). Namely, proteinase K pretreatment enhanced the detectability, and the suitable concentration of the labeled antigen solution ranged from 50 to 100 μg/mL.
2. In the rat experiment, Ag53 antibodies were demonstrated only in the animals immunized with the Ag53-positive bacterial strain. In human cases, antibodies against Ag53 were undetectable in both the sera and tissues. The lack of anti-Ag53 antibody reaction in humans may be explained as follows: The infection of Ag53-positive *P. gingivalis* is not as frequent as expected in human lesions, or Ag53 is pathogenic in periodontitis but not in dental caries–associated radicular cyst.
3. In both rat and human, the Arg-hgp and Lys-hgp portions of *P. gingivalis*–derived gingipains were immunogenic when compared with the Arg-pro and Lys-pro portions. Reportedly, in patients with periodontitis, serum antibodies to Arg-hgp were raised (O'Brien-Simpson et al. 2000; Inagaki 2001), whereas antibodies to Arg-pro were not provoked (Inagaki 2001). In contrast, serum antibodies immunoprotective against *P. gingivalis* infection were detected when mice were experimentally immunized with synthetic peptides from Arg-pro (Genco et al. 1998; O'Brien-Simpson et al. 2001).
4. In patients 3 and 6, anti-Arg-hgp and anti-Lys-hgp antibodies were detected in CD138-positive plasma cells accumulated in the gingival tissue but not in the serum. It is hypothesized that these antibodies were produced locally but not secreted into the blood. The fact indicates the importance of evaluating the diseased tissue itself with this novel histochemical technique, the enzyme-labeled antigen method.
5. The pathogenetic significance of *P. gingivalis* infection in radicular cyst remains to be solved since only 2 of 10 lesions evaluated showed the production of anti-gingipain antibodies. *P. gingivalis* has so far been isolated from the root canal and the lesion of radicular cyst (Jung et al. 2000; Dahlen 2002; Wayman et al. 2002; Sunde et al. 2003; Noguchi et al. 2005), but the isolation is inconsistent: Noguchi et al. (2005) reported that biofilm infection of *P. gingivalis* was associated with refractory periapical periodontitis. Jung et al. (2000) reported that *P. gingivalis* was isolated from 26.3% of root canal infection and that *P. gingivalis* infection was significantly related to symptom manifestation. Our data suggest that infection of *P. gingivalis* and immune reaction to this pathogen may be involved in the pathogenesis of part (one-fifth) of the radicular cyst lesions.
6. Another question is the reason why the elevated serum antibody titers against gingipains were demonstrated in two cases, in which plasma cells were scarcely infiltrated in frozen sections of radicular cyst (although one of these two lesions showed plasma cell infiltration in paraffin sections). It may be related to the complication of periodontitis, because both of these cases showed a moderate degree of periodontal bone absorption.
7. Antibodies to SpaP of *S. mutans* origin were undetectable in the patients' sera and radicular cyst lesions, except for one case (case 8) in which serum antibody titer against SpaP was elevated. We should explain the reason for such unexpected negative data on the dental caries–causing bacteria by continuing further analysis.
8. We should discuss the specificity of the method. The absorption experiment using an excess amount of unlabeled antigens supported the specificity of the present technique, we believe. In rat and human tissues, antibodies against the epitope common between Arg-hgp and Lys-hgp were produced in a good number of plasma cells, whereas the other plasma cells contained antibodies specific to epitopes unique in either Arg-hgp or Lys-hgp. In fact, the homology of the amino acid sequence of both domains is estimated 76% (758/1007) (O'Brien-Simpson et al. 2001). According to the protein sequence analysis using the Basic Local Alignment Search Tool (BLAST),

the homology between Arg-pro and Lys-pro was 30% (148/501). Lower homology data were observed among the other antigens examined, although regional short segment homology was seen: for example, 73% (40/55) between Arg-hgp and Lys-pro, 55% (19/35) between Arg-hgp/Lys-hgp and Arg-pro, and 24% (16/67) between Ag53 and Arg-hgp/Lys-hgp. It is intriguing to say that the region (or epitope) specificity was able to be shown with our histochemical technique. When the difference in the amino acid sequence is considered, Ag53 and gingipains can be regarded as indifferent antigens, and hgp and pro regions in gingipains also belong to indifferent proteins for each other.

9. It may happen that the specific antibodies demonstrated in plasma cells in rat and human tissues belong to immunoglobulins that were originally raised against closely related proteins coming from different bacteria. To exactly confirm the specificity of the antibodies detected in tissue sections, we should extend our study to perform bacterial isolation from the diseased tooth root and radicular cyst lesions, and antigens cross-reactive to Ag53 or gingipain domains should be screened in *P. gingivalis*–related or unrelated pathogens by analyzing the gene database. When labeled antigens strictly specific to certain pathogens are not available or their strict specificity is unknown, the positive findings with plural probes may strengthen the specificity in the enzyme-labeled antigen method, as in the present study and also for the immunoperoxidase technique.

To use the enzyme-labeled antigen method as a ubiquitous technique, one must consider the method of preparing labeled antigens.

When the pathogenic proteins are known, the sequence of transcription of DNA to yield mRNA and translation of mRNA to yield protein products can be introduced. The cell-free protein synthesis system employing the wheat germ extract gives an efficient tool for this purpose (Sawasaki, Hasegawa, et al. 2002; Sawasaki, Ogasawara, et al. 2002). Once the plasmid construction is ready, crude or purified biotinylated proteins can be synthesized automatically within 36 hr.

For preparing the labeled antigens for analyzing autoimmune diseases in which the pathogenic antigens are not necessarily known, human/mouse libraries of autoimmune-related antigens are useful: The Cell-Free Science and Technology Research Center at Ehime University has established those libraries containing more than 2000 biotinylated proteins by applying the cell-free protein synthesis system (Matsuoka K, Endo Y, Sawasaki T, unpublished data). The target antigens can be screened in the human library with the patient's serum and diseased tissue extract: The AlphaScreen method is quite suitable for this purpose (Matsuoka et al. 2010).

In conclusion, the significance of our idea on the enzyme-labeled antigen method includes the following:

1. The target antigens (or even epitopes) of the antibodies produced within the lesion are detectable, so that the pathogenesis of the lesion can be analyzed in view of the site of antibody production.
2. Analysis of the serum and tissue extract with the AlphaScreen method provides the specificity confirmation of this novel histochemical technique.
3. The method for preparing labeled probes for the enzyme-labeled antigen method, the wheat germ extract–mediated cell-free protein synthesis system, is relatively simple and automated, so that the site of antibody production can be visualized specifically by applying this technique.
4. Our approach is applicable to a variety of lesions with plasma cell infiltration and provides a novel histochemical tool for analyzing disease process.

The possible target lesions of the enzyme-labeled antigen method include 1) the autoimmune diseases, such as rheumatoid arthritis, Hashimoto thyroiditis, Sjögren syndrome, ulcerative colitis, and autoimmune gastritis; 2) infectious diseases, such as *Helicobacter pylori*–induced gastritis and syphilis; and 3) malignant tumors showing heavy infiltration of plasma cells in the stroma, including Epstein-Barr virus–related tumors (nasopharyngeal carcinoma, gastric carcinoma with lymphoid stroma, Hodgkin's lymphoma, and nasal malignant lymphoma), human papilloma virus–related uterine cervical carcinoma, mucosa-associated lymphoid tissue lymphoma, and multiple myeloma (plasmacytoma).

We sincerely hope that the enzyme-labeled antigen method is widely used as a novel histochemical technique.

Acknowledgments

Skillful technical assistance by Ms. Hisayo Ban, Ms. Mai Ito, and Ms. Mika Maeshima and effective office work by Ms. Chikayo Yashiro, Department of Pathology, Fujita Health University School of Medicine, Toyoake, are cordially appreciated. Prof. Hideki Mizutani, Department of Oral and Maxillofacial Surgery, Fujita Health University School of Medicine, Toyoake, kindly gave us valuable advice and suggestions. We appreciate Mr. Ryo Morishita, CellFree Science, Matsuyama, Japan, for his technical contribution to the AlphaScreen method and bacterial protein purification.

Declaration of Conflicting Interests

The author(s) declared no potential conflicts of interest with respect to the authorship and/or publication of this article.

Funding

The author(s) disclosed receipt of the following financial support for the research and/or authorship of this article: This work was supported by the Grant from the Ministry of Education, Culture, Sports, Science and Technology, Japan (#17390106 and #18659103 to Y.T. and #21890277 to Y.M.) and also in part by the Research Grant from Fujita Health University (2006 to Y.T.).

References

Chen T, Nakayama K, Belliveau L, Duncan MJ. 2001. *Porphyromonas gingivalis* gingipains and adhesion to epithelial cells. Infect Immun. 69:3048–3056.

Cutler CW, Calmer JR, Genco CA. 1995. Pathogenic strategies of the oral anaerobe, *Porphyromonas gingivalis*. Trends Microbiol. 3:45–51.

Dahlen G. 2002. Microbiology and treatment of dental abscesses and periodontal-endodontic lesions. Periodontol 2000. 28: 206–239.

Feder JN, Assaraf YG, Seamer LC, Schimke RT. 1989. The pattern of dihydrofolate reductase expression through the cell cycle in rodent and human cultured cells. J Biol Chem. 264:20583–20590.

Galaviz LAA, Medina MDCA, García ICE. 2002. Detection of potentially cariogenic strains of *Streptococcus mutans* using the polymerase chain reaction. J Clin Pediatr Dent. 27:47–51.

Genco CA, Odusanya BM, Potempa J, Mikolajczyk-Pawlinska J, Travis J. 1998. A peptide domain on gingipain R which confers immunity against *Porphyromonas gingivalis* infection in mice. Infect Immun. 66:4108–4114.

Grenier D, Tanabe S. 2010. *Porphyromonas gingivalis* gingipains trigger a proinflammatory response in human monocyte-derived macrophages through the p38α mitogen-activated protein kinase signal transduction pathway. Toxins. 2:341–352.

Guentsch A, Kramesberger M, Sroka A, Pfister W, Potempa J, Eick S. 2011. Comparison of gingival crevicular fluid sampling methods in patients with severe chronic periodontitis. J Periodontol. 79:119–132.

Holt SC, Kesavalu L, Walker S, Genco CA. 1999. Virulence factors of *Porphyromonas gingivalis*. Periodontol 2000. 20:168–238.

Inagaki S. 2001. Antibody responses to Arg-gingipain of *Porphyromonas gingivalis* in periodontitis patients [in Japanese with English abstract]. Nihon Shishubyo Gakkai Kaishi. 43:240–250.

Jung I-Y, Choi B-K, Kum K-Y, Roh B-D, Lee S-J, Lee C-Y, Park D-S. 2000. Molecular epidemiology and association of putative pathogens in root canal infection. J Endod. 26:599–604.

Kato T, Tsuda T, Inaba H, Kawai S, Okahashi N, Shibata Y, Abiko Y, Amano A. 2008. *Porphyromonas gingivalis* gingipains cause G(1) arrest in osteoblastic/stromal cells. Oral Microbiol Immun. 23:158–164.

Kurihara H, Nishimura F, Nakamura T, Nakagawa M, Tanimoto I, Nomura Y, Kokeguchi S, Kato K, Murayama Y. 1991. Humoral immune response to an antigen from *Porphyromonas gingivalis*381 in periodontal disease. Infect Immun. 59:2758–2762.

Lamont RJ, Jenkinson HF. 1998. Life below the gum line: pathogenic mechanisms of *Porphyromonas gingivalis*. Microbiol Mol Biol Rev. 62:1244–1263.

Leduc EH, Avrameas S, Bouteille M. 1968. Ultrastructural localization of antibody in differentiating plasma cells. J Exp Med. 127:109–118.

Lee SF, Progulske-Fox A, Bleiweis AS. 1988. Molecular cloning and expression of a *Streptococcus mutans* major surface protein antigen, P1 (I/II), in *Escherichia coli*. Infect Immun. 56:2114–2119.

Matsuoka K, Komori H, Nose M, Endo Y, Sawasaki T. 2010. Simple screening method for autoantigen proteins using the *N*-terminal biotinylated protein library produced by wheat cell-free synthesis. J Proteome Res. 9:4264–4273.

Mizutani Y, Tsuge S, Shiogama K, Shimomura R, Kamoshida S, Inada K, Tsutsumi Y. 2009. Histochemical detection of antigen-specific antibody-producing cells in tissue sections of rats immunized with horseradish peroxidase, ovalbumin or keyhole limpet hemocyanin. J Histochem Cytochem. 57:101–111.

Naito M, Hirakawa H, Yamashita A, Ohara N, Shoji M, Yukitake H, Nakayama K, Toh H, Yoshimura F, Kuhara S, et al. 2008. Determination of the genome sequence of *Porphyromonas gingivalis* strain ATCC 33277 and genomic comparison with strain W83 revealed extensive genome rearrangements in *P. gingivalis*. DNA Res. 15:215–225.

Noguchi N, Noiri Y, Narimatsu M, Ebisu S. 2005. Identification and localization of extraradicular biofilm-forming bacteria associated with refractory endodontic pathogens. Appl Environ Microbiol. 71:8738–8743.

O'Brien-Simpson NM, Black CL, Bhogal PS, Cleal SM, Slakeski N, Higgins TJ, Reynolds EC. 2000. Serum immunoglobulin G (IgG) and IgG subclass responses to the RgpA-Kgp proteinase-adhesin complex of *Porphyromonas gingivalis* in adult periodontitis. Infect Immun. 68:2704–2712.

O'Brien-Simpson NM, Paolini RA, Reynolds EC. 2001. RgpA-Kgp peptide-based immunogens provide protection against *Porphyromonas gingivalis* in a murine lesion model. Infect Immun. 68:4055–4063.

Oyaizu K, Ohyama H, Nishimura F, Kurihara H, Matsushita S, Maeda H, Kokeguchi S, Hongyo H, Takashiba S, Murayama Y. 2001. Identification and characterization of B-cell epitopes of a 53-kDa outer membrane protein from *Porphyromonas gingivalis*. Oral Microbiol Immunol. 16:73–78.

Sawasaki T, Hasegawa Y, Tsuchimochi M, Kamura N, Ogasawara T, Kuroita T, Endo Y. 2002. A bilayer cell-free protein synthesis system for high-throughput screening of gene products. FEBS Lett. 514:102–105.

Sawasaki T, Kamura N, Matsunaga S, Saeki M, Tsuchimochi M, Morishita R, Endo Y. 2008. Arabidopsis HY5 protein functions as a DNA-binding tag for purification and functional immobilization of proteins on agarose/DNA microplate. FEBS Lett. 582:221–228.

Sawasaki T, Ogasawara T, Morishita R, Endo Y. 2002. A cell-free protein synthesis system for high-throughput proteomics. Proc Natl Acad Sci U S A. 99:14652–14657.

Schenkein HA. 2006. Host responses in maintaining periodontal health and determining periodontal disease. Periodontol 2000. 40:77–93.

Sebestyén A, Berczi L, Mihalik R, Paku S, Matolcsy A, Kopper L. 1999. Syndecan-1 (CD138) expression in human non-Hodgkin lymphomas. Br J Haematol. 104:412–419.

Slots J, Ting M. 1999. *Actinobacillus actinomycetemcomitans* and *Porphyromonas gingivalis* in human periodontal disease: occurrence and treatment. Periodontol 2000. 20: 82–121.

Straus W. 1968. Cytochemical detection of sites of antibody to horseradish peroxidase in spleen and lymph nodes. J Histochem Cytochem. 16:237–248.

Sunde PT, Olsen I, Göbel UB, Theegarten D, Winter S, Debelian GJ, Tronstad L, Moter A. 2003. Fluorescence in situ hybridization (FISH) for direct visualization of bacteria in periapical lesions of asymptomatic root-filled teeth. Microbiology. 149:1095–1102.

Wayman BE, Murata SM, Almeida RJ, Fowler CB. 1992. A bacteriological and histological evaluation of 58 periapical lesions. J Endod. 18:152–155.

Xu Z, Nagashima K, Sun D, Rush T, Northrup A, Andersen JN, Kariv I, Bobkova EV. 2009. Development of high-throughput TR-FRET and AlphaScreen assays for identification of potent inhibitors of PDK1. J Biomol Screen. 14:1257–1262.

Yoshida A, Kuramitsu HK. 2002. *Streptococcus mutans* biofilm formation: utilization of a gtfB promoter-green fluorescent protein (PgtfB:gfp) construct to monitor development. Microbiology. 148:3385–3394.

FEBS Letters 585 (2011) 1835–1840

ELSEVIER

FEBS Letters

journal homepage: www.FEBSLetters.org

Caspase-8 cleavage of the interleukin-21 (IL-21) receptor is a negative feedback regulator of IL-21 signaling

Tatsuya Akagi [a], Kouhei Shimizu [a], Shoukichi Takahama [b], Takahiro Iwasaki [b], Kazuhiro Sakamaki [c], Yaeta Endo [a,b,d,e,*], Tatsuya Sawasaki [a,b,d,e,*]

[a] Cell-Free Science and Technology Research Center, Ehime University, 3 Bunkyo-cho, Matsuyama, Ehime 790-8577, Japan
[b] The Venture Business Laboratory, Ehime University, 3 Bunkyo-cho, Matsuyama, Ehime 790-8577, Japan
[c] Department of Animal Development and Physiology, Graduate School of Biostudies, Kyoto University, Kyoto 606-8501, Japan
[d] Proteo-Medicine Research Center, Ehime University, Toon, Ehime 791-0295, Japan
[e] RIKEN Systems and Structural Biology Center, 1-7-22 Suehiro-cho, Tsurumi, Yokohama 230-0045, Japan

ARTICLE INFO

Article history:
Received 1 February 2011
Revised 5 April 2011
Accepted 13 April 2011
Available online 20 April 2011

Edited by Vladimir Skulachev

Keywords:
Caspase-8
Cell-free system
Interleukin-21
Cytokines
Apoptosis

ABSTRACT

We screened a library of human single-transmembrane proteins (sTMPs), produced by a cell-free system, using a luminescent assay to identify those that can be cleaved by caspase-8 (CASP8). Of the 407 sTMPs screened, only the interleukin-21 receptor (IL21R), vezatin (VEZT), and carbonic anhydrase XIV were cleaved at Asp344, Asp655 and Asp53, respectively. We confirmed that IL21R and VEZT were also cleaved in apoptotic HeLa cells with the cleavage sites. Interestingly, IL21R was cleaved within 30 min after apoptosis induction. Furthermore the CASP8-cleaved form of IL21R did not induce phosphorylation at Tyr705 of STAT3. Our results suggest that the interleukin-21 signaling cascade is negatively regulated by CASP8.

1. Introduction

Procaspase-8 (proCASP8) is part of the trans-plasma membrane death-inducing signaling complex and is located on the cytosolic side [1]. Binding of extracellular ligands, e.g., the FAS ligand, to the death inducing signaling complex activates proCASP8, which is then released from the complex as caspase-8 (CASP8). Pro-apoptotic proteins, e.g., caspase-3 (CASP3) and the BH3 interacting domain death agonist (Bid), are cleaved by CASP8 as part of the apoptotic pathway. These CASP8 substrates are found in the cytosol. However, there have been reports that CASP8 cleaves membrane-bound v-erb-b2 erythroblastic leukemia viral oncogene homolog 2 (ERBB2) in apoptotic cells [2] and also interacts with other membrane proteins [3,4]. These reports show that CASP8 can cleave membrane proteins. Identification of CASP8-cleavable membrane proteins would therefore increase our knowledge of their functions.

We have developed a high-throughput, automated protein production method that uses a wheat cell-free system [5,6], and this system has been used to construct an in vitro-expressed proteome composed of 13 364 human proteins [7] and a kinase library for which the kinases are N- and C-terminally tagged (NCtagged) with the Flag sequence and biotin, respectively [8]. The kinase library, in conjunction with a commercially available assay system that measures luminescence (AlphaScreen), was used to identify substrates of CASP3. Interestingly, of the 13 364 proteins found in the proteome, 1320 are single transmembrane proteins (sTMPs), i.e., those with a single transmembrane (sTM) region, such as ERBB2. For the study reported herein, we adapted the assay system for use with a human NCtagged sTMP library generated by our cell-free system to screen for CASP8-cleavable sTMPs. Interleukin-21 receptor (IL21R) was found to be a CASP8 substrate, and its cleavage by

Abbreviations: Bid, BH3 interacting domain death agonist; CA14, carbonic anhydrase XIV; CASP8, caspase-8; ERBB2, v-erb-b2 erythroblastic leukemia viral oncogene homolog 2; IL-21, interleukin-21; IL21R, interleukin-21 receptor; IL2RG, interleukin 2 receptor, gamma; NCtagged, N- and C-terminally tagged; sTMP, single transmembrane protein; sTMG, single transmembrane gene; VEZT, vezatin

* Corresponding authors at: Cell-Free Science and Technology Research Center, Ehime University, 3 Bunkyo-cho, Matsuyama, Ehime 790-8577, Japan. Fax: +81 89 927 9941.

E-mail addresses: yendo@eng.ehime-u.ac.jp (Y. Endo), sawasaki@ehime-u.ac.jp (T. Sawasaki).

0014-5793/$36.00 © 2011 Federation of European Biochemical Societies. Published by Elsevier B.V. All rights reserved.
doi:10.1016/j.febslet.2011.04.031

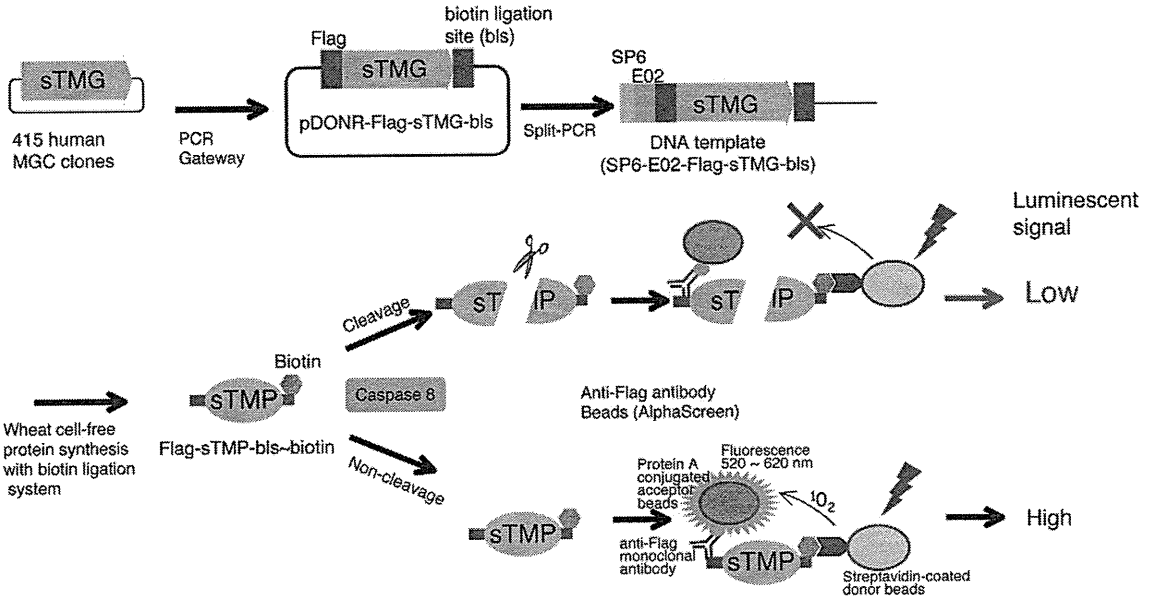

Fig. 1. Strategy for screening sTMPs cleaved by CASP8. Genes having a single transmembrane region (sTM) were selected from the human MGC library.

CASP8 in vivo suggests that CASP8 is a negative feedback regulator of interleukin-21 (IL-21) signaling.

2. Materials and methods

2.1. General

The following procedures have either been described in detail or cited [5,6,8–10]: generation of DNA templates by PCR using split-primers; parallel syntheses of mRNAs and proteins; biotin labeling of the proteins; amino acid sequencing; immunoblotting detection and luminescent detection of caspase cleavage. Anti-Flag and anti-V5 antibodies were purchased from Sigma–Aldrich (St. Louis, MO) and Invitrogen (Carlsbad, CA), respectively. Antibodies specific for endogenous Bid, cleaved PARP, tubulin, STAT3, and STAT3 phosphorylated at Tyr705 were purchased from Cell Signaling Technology (Beverly, MA).

2.2. Construction of DNA templates

The single transmembrane genes (sTMGs) used in this study are listed in Supplementary Table 1. Methods for construction of pDONR-Flag-sTMG-bls plasmids were based on previous report [8]. Genes for expression in the cell were inserted into a pcDNA3.2/V5-DEST by the Gateway method (Invitrogen). The interleukin 2 receptor, gamma (IL2RG) (GenBank Accession No. BC014972) and JAK3 (BC028068) genes from MGC clones were each inserted into a pcDNA3.1 vector to construct pcDNA3.1-IL2RG-Flag and pcDNA3.1-JAK3-myc vectors, respectively. The pcDNA3.2-C8M-IL21R vector was constructed by inserting the IL21R nucleotide sequence corresponding to residues 1–344 into the pcDNA3.2 vector. D → A mutagenesis was carried out using the reagents of a PrimeSTAR Mutagenesis Basal kit (TakaraBio, Otsu, Japan) according to the manufacturer's instructions.

2.3. Cell-free protein synthesis

The sTMPs were produced using the robotic synthesizer GenDecoder 1000 (CellFree Sciences, Yokohama, Japan) and the reagents of ENDEXT kits, i.e., the wheat cell-free system (CellFree Sciences), biotin ligase, and biotin [6,8,9].

2.4. Cleavage assay using the luminescent method and immunoblotting

For each sTMP, 10 μl of the CASP8-cleavage buffer [6.7 mM Tris–HCl, pH 7.5, 167 mM NaCl, 0.8 mM EDTA, 3.3 mM DTT, 3.3% glycerol, 0.03% CHAPS, and 1 U CASP8 (Sigma–Aldrich)] was mixed with 1 μl of the translation mixture that contained a Flag-sTMP-bls~biotin construct, and the mixture was incubated at 30 °C for 2 h in a well of a 384-well Optiplate (Perkin Elmer, Foster City, CA).

2.5. Amino acid sequences of the CASP8 cleavage sites

For IL21R and carbonic anhydrase XIV (CA14), their biotinylated C-terminal fragments produced by CASP8 cleavage were recovered while attached to streptavidin beads and then sequenced directly. For vezatin (VEZT), C-terminally GST fused VEZT was used.

2.6. Cell-based assay

HeLa and Jurkat cells [wild-type (A3, ATCC, Riken Cell Bank, Tsukuba, Japan; CRL-2570) and CASP8-deficient (I9.2, ATCC CRL-2571)] were grown in Dulbecco's modified eagle medium (DMEM) and RPMI medium, respectively, 10% fetal bovine serum (FBS), penicillin (100 mg/ml), and streptomycin (50 μg/ml). Twenty-four hours after transfection, cells were harvested after apoptosis had been induced. For apoptosis induction or inhibition, with 200 ng/ml anti-Fas antibody (Medical and Biological Laboratories Co. Ltd., Nagoya, Japan) in the presence (inhibition) or absence (induction) of 50 μM Z-IETD-FMK (Calbiochem, San Diego, CA) or 50 μM Z-VAD-FMK (Peptide Institute Inc., Osaka, Japan) for 6 h. For analysis of the IL-21 signaling pathway, pcDNA3.2-IL21R or pcDNA3.2-C8M-IL21R vector was cotransfected into HeLa cells with pcDNA3.1-IL2RG-Flag and pcDNA3.2-HA-JAK3 vectors. The cells were treated with 50 ng/μl IL-21 for 30 min, after 24 h of transfection.

3. Results

3.1. Generation of an NCtagged sTMP library for screening of CASP8 substrates

First, we examined the 9362 full-length human gene sequences of the Mammalian Gene Collection (MGC) (http://www.mgc.nci.nih.gov/) to find sTMP sequences using the predictive program TMHMM version 2.0 (http://www.cbs.dtu.dk/services/TMHMM/), and then we classified the sTMG according to the terms used in the Gene Ontology (GO) database (http://www.geneontology.org/). In the end, 574 independent genes having a single transmembrane region were selected and their sequences used to make an NCtagged sTMP library. The NCtagged sTMPs were produced using the wheat cell-free system and an automatic GenDecorder 1000 in the presence of biotin and biotin ligase [8,9] (Fig. 1). Then, 407 human sTMPs, i.e., those with luminescence signals >500 units, were selected for the final sTMP library (Supplementary Table 1). To check the performance of the assay system, we used Bid and ERBB2, which are known as CASP8 substrates [2,11]. Flag-Bid-bls~biotin and Flag-ERBB2-bls~biotin were each treated with active CASP8 and their cleavage by CASP8 was first confirmed by immunoblotting with Alexa488-labeled streptavidin (Fig. 2A). Furthermore, the two NCtagged substrates were used for luminescent assay. After CASP8 treatment, the strengths of the luminescent signals of the two protein samples decreased; whereas that of a non-cleavable, control protein (*Escherichia coli* dihydrofolate reductase) did not (Fig. 2B). These results showed that the assay system could be used to detect CASP8-cleavable NCtagged sTMPs in place of or as an adjunct to conventional immunoblotting.

3.2. Screening for CASP8-cleavable sTMPs in the sTMP library

Using the luminescent detection assay, the proteins of the NCtagged sTMP library were screened for CASP8 cleavability (Fig. 2C). The signals for three sTMPs were <65% of their initial signals; whereas, the signals of the other 404 sTMPs were not or were less affected by CASP8 treatment. For the three sTMPs with luminescent signals affected by CASP8, both a general caspase (z-VAD-FMK) and a CASP8-specific (z-IETD-FMK) inhibitor prevented the signal reduction caused by the presence of CASP8 (Fig. 2D). The cleavage of the three sTMPs by CASP8 was confirmed by conventional immunoblotting using anti-Flag antibodies and fluorescent streptavidin (Fig. 3A). The CASP8-cleavage sites in the three proteins were identified by amino acid sequencing of their cleaved C-terminal fragments (Fig. 3B). The cleavage sites of IL21R, VEZT, and CA14 were VESD↓G_{344}, PQAD↓G_{705}, and IQTD↓S_{53}, respectively, which are consensus-type sequences [X-E/Q-X-D↓-G/S (X is any amino acid and ↓ is the cleavage site, http://www.merops.sanger.ac.uk)]. We also found identical or similar sites in orthologous mammalian proteins (Fig. 3B), indicating that these sites may be conserved among mammals.

3.3. Characterization of the CASP8-cleavable sTMPs in HeLa cells made apoptotic by anti-Fas antibodies

We investigated whether the sTMPs found to be cleaved by CASP8 in vitro were also cleaved in HeLa cells made apoptotic by anti-Fas antibodies. Expression of IL21R-V5 and VEZT-V5 was detected in the transfected cells; whereas, CA14-V5 was not expressed. In apoptotic cells, cleavage of the two sTMPs occurred

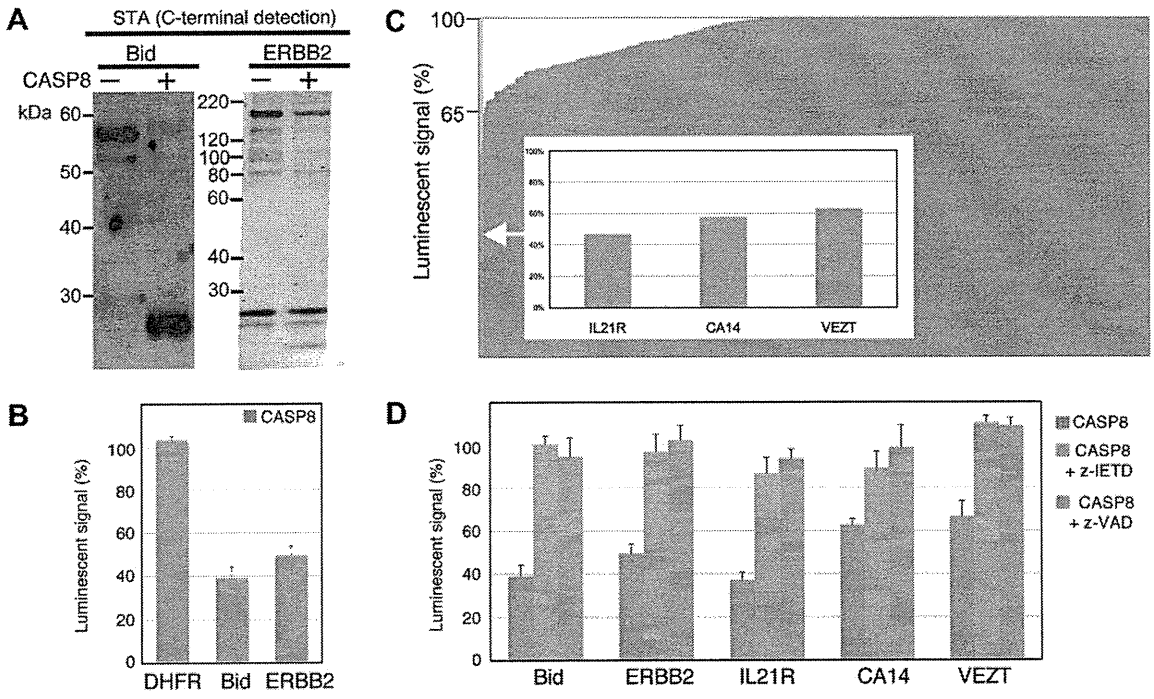

Fig. 2. Screening for CASP8-cleaved sTMP substrates using the NCtagged sTMP library. (A) Immunoblot of NCtagged Bid and ERBB2 that had been incubated in the presence (+) or absence (–) of CASP8. Alexa488-labeled streptavidin (STA) was used for detection. (B) Detection of CASP8-cleaved NCtagged Bid and ERBB2 using the AlphaScreen luminescence system. The luminescence for the controls (no CASP8) was set to 100%. (C) Relative luminescent signals after in vitro CASP8 treatment of NCtagged sTMPs that had been synthesized in the wheat cell-free system. The *x* axis lists the NCtagged sTMPs in ascending order of their luminescent signals after CASP8 treatment. NCtagged sTMPs that returned luminescent signals <65% of the control values (green rectangle) are identified in the inset along with their relative luminescent signals. (D) Inhibition assay using the AlphaScreen.

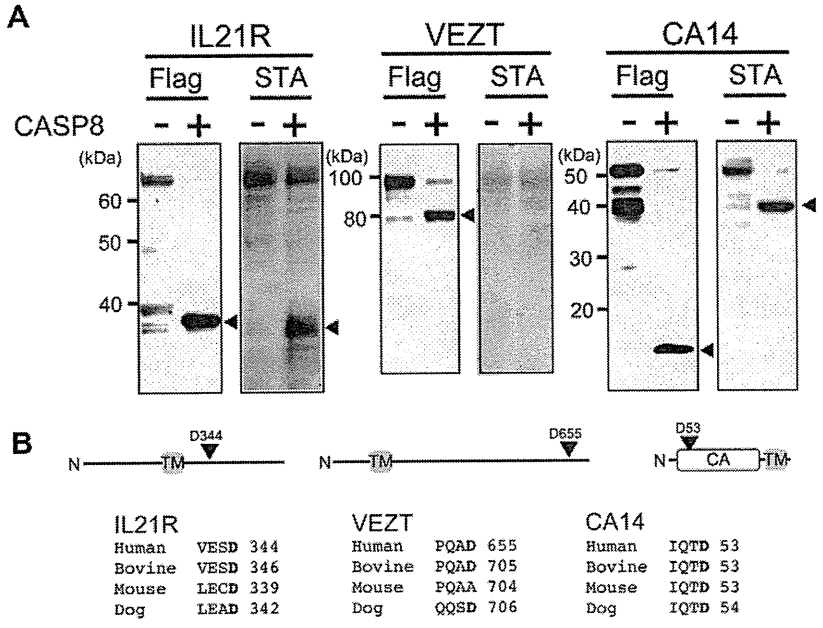

Fig. 3. In vitro cleavage of sTMPs by CASP8. (A) The NCtagged sTMPs were incubated in the presence (+) or absence (−) of CASP8 and their cleavage products (solid arrowheads) were detected using anti-Flag antibodies (Flag) and Alexa488-conjugated streptavidin (STA), which bound to the N- and C-termini of the sTMP constructs, respectively. (B) Sequence alignments of the CASP8-cleavage sites for the three sTMPs are shown at the bottom of the figure.

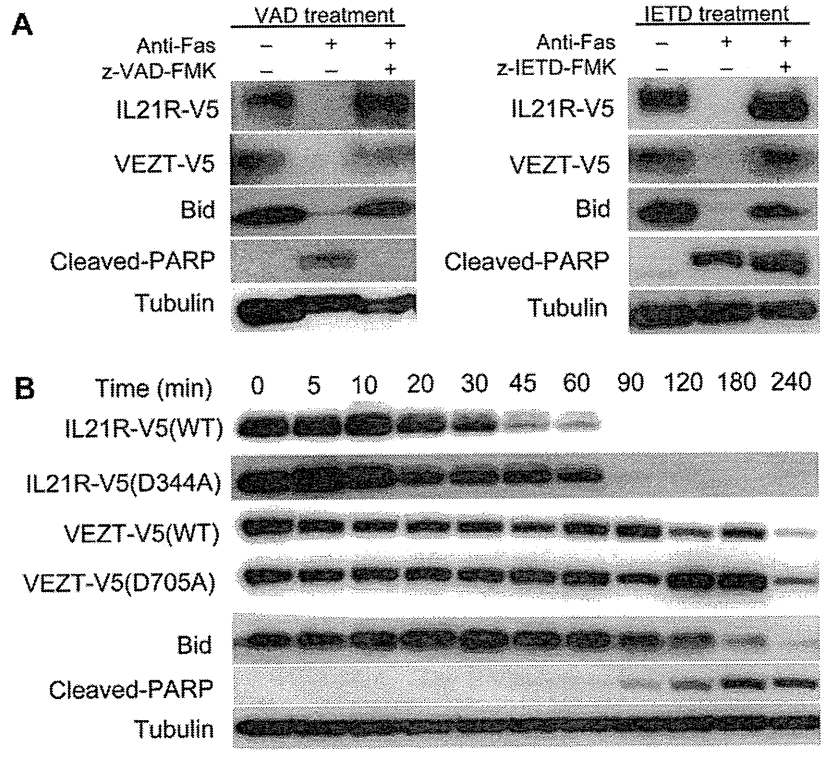

Fig. 4. Cleavage of two of the newly identified sTMP substrates in the apoptotic cells. (A) The cells were treated with DMSO (control), or with anti-Fas antibodies in the presence or absence of z-VAD-FMK or z-IETD-FMK for 6 h and then lysed. (B) Time course for the expression of IL21R and VEZT in apoptotic HeLa cells. IL21R-V5 (wild type, WT), the D344A mutant of IL21R-V5, VEZT-V5 (WT), and the D705A mutant of VEZT-V5 were expressed in apoptotic HeLa cells.

and was completely blocked by z-VAD-FMK and z-IETD-FMK (Fig. 4A). Therefore, our approach, using the sTMP library, identified two new in vivo targets of CASP8.

We investigated some of the events that occurred shortly after IL21R cleavage by CASP8 in apoptotic HeLa cells. Importantly, although IL21R cleavage was detected at 30 min after apoptosis induction using anti-Fas antibodies (and it was almost entirely complete within 90 min) (Fig. 4B), VEZT cleavage was nearly complete only 2 h after apoptotic induction. In vivo cleavage of Bid and PARP (poly (ADP-ribose) polymerase 1) have, respectively, been

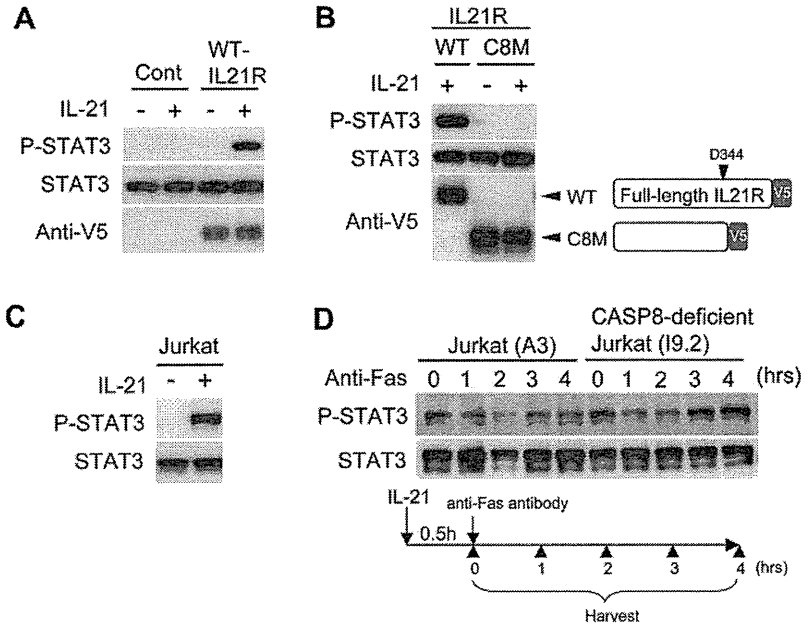

Fig. 5. Characterization of in vivo CASP8-cleaved IL21R (A) HeLa cells Cells were treated with (+) or without (−) IL21 for 1 h after 24 h of transfection and then lysed. Endogenous STAT3 and STAT phosphorylated at Tyr705 (P-STAT3) were detected by antibodies specific for each protein. (B) pcDNA3.1-IL2RG-Flag and pcDNA3.2-HA-JAK3 constructs were expressed with pcDNA3.2-IL21R (WT) or pcDNA3.2-C8M-IL21R (C8M), which is a truncated form that mimics the CASP8-cleaved form. (C) Jurkat cells were treated with (+) or without (−) IL21 for 1 h. (D) Jurkat (A3) and CASP8-deficient Jurkat I9.2 cells were treated with IL21 for 0.5 h and then treated with anti-Fas antibody.

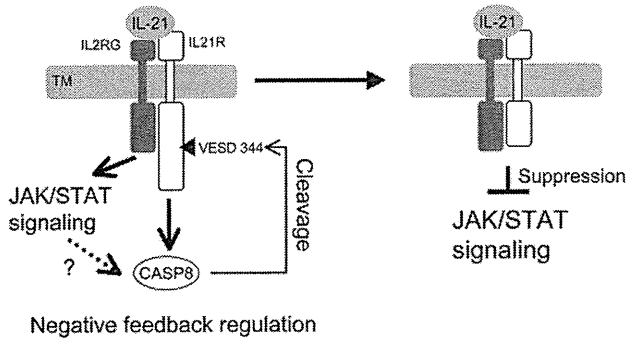

Fig. 6. Model for negative feedback regulation of IL-21 by CASP8 cleavage of IL21R.

used as indicators of CASP8 and caspase-3 activation. Our finding that IL21R is cleaved by CASP8 during initiation phase of apoptosis is consistent with that of previous work, which showed that CASP8 was activated 30 min within the onset of apoptosis [12].

3.4. A biological function for CASP8-cleaved IL21R

IL21 activates the JAK/STAT signaling cascade by forming a complex between IL2RG (IL2Rγ) and IL21R [13,14], and IL-21 also induces apoptosis in B cells [15]. Because STAT3 phosphorylation at Tyr705 is part of the signaling cascade initiated by IL-21 [14], we first attempted to determine the phosphorylation state of Tyr705 in STAT3 when CASP8 was inhibited with a CASP8-specific (z-IETD-FMK) inhibitor in vivo. However, z-IETD-FMK inhibited STAT3 phosphorylation in the absence of CASP8 (data not shown). Therefore, to investigate the biological function of the caspase-cleaved IL21R, we reconstructed the IL-21-dependent JAK/STAT signaling by coexpression of IL21R, JAK3, and IL2RG in HeLa cells. When all three genes were transfected into the cells, STAT3 phosphorylation at Tyr 705 occurred (Fig. 5A). Then, the gene for C8M-IL21R, a truncated form of IL21R (residues 1–344) that mimics the CASP8-cleaved IL21R, was transfected with the genes for JAK3 and IL2RG. However, STAT3 phosphorylation was not observed in the cells although C8M-IL21R was expressed (Fig. 5B), suggesting that CASP8 cleavage of IL21R may block JAK/STAT signaling. Furthermore, because IL-21 induced STAT3 phosphorylation in Jurkat cells (Fig. 5C), normal Jurkat (A3) and Jurkat (I9.2) cells lacking CASP8 activity [4,16] were used to assess IL-21-induced STAT3 signaling after CASP8 activation. After IL-21 treatment for 0.5 h, normal Jurkat and I9.2 cells were made apoptotic by anti-Fas antibodies. In normal Jurkat cells, STAT3 phosphorylation decreased within 4 h. In contrast, in I9.2 cells, STAT3 remained phosphorylated at least up to 4 h after apoptosis was induced (Fig. 5D). Therefore, CASP8 cleavage of IL21R may inhibit IL-21-dependent JAK/STAT signaling.

4. Discussion

The involvement of capsases in interleukin signaling pathway(s) has not been fully delineated. As one intriguing example, caspase-1 processes the proinflammatory cytokine, proIL-1β, into mature IL-1β [17], which implies that at least one caspase is part of an interleukin signaling pathway. In the NCtagged sTMP library, two interleukins (IL-8 and IL-27) and eight interleukin receptors (IL1R2, IL2RG, IL3RA, IL10RB, IL11RA, IL21R, IL22RA1, and IL27RA) were included. However, CASP8 cleaved only IL21R as shown by both the luminescent assay and immunoblotting. Therefore, possibly only IL-21 signaling may be directly related to CASP8 activation. The IL-21 signaling pathway is a modulator of lymphoid proliferation, apoptosis, and differentiation [18]. CASP8 is involved in lymphocyte proliferation and differentiation [19]. Interestingly, in B cells, IL-21 mediated apoptosis involved activation of CASP8 and CASP3, which may be caused by high expression of IL21R via CD40 stimulation [20,21]. In the presence of exogenous IL-21, the CASP8-cleaved form of IL21R did not induce the phosphorylation of Tyr 705 in STAT3 (Fig. 5B), and CASP8 cleavage of IL21R, as part of the apoptosis process, reduced the phosphorylation (Fig. 5D). A

previous study showed that IL-21 induces proliferation of human myeloma cells through tyrosine phosphorylation of STAT3 [22]. Taken together, as shown in Fig. 6, CASP8 appear to act as negative feedback regulators of IL-21 signaling by their cleavage of IL21R.

Acknowledgments

This work was partially supported by the Special Coordination Funds for Promoting Science and Technology by the Ministry of Education, Culture, Sports, Science and Technology, Japan (Nos. 19657041 and 22310127 to T.S.).

Appendix A. Supplementary data

Supplementary data associated with this article can be found, in the online version, at doi:10.1016/j.febslet.2011.04.031.

References

[1] Muzio, M. et al. (1996) FLICE, a novel FADD-homologous ICE/CED-3-like protease, is recruited to the CD95 (Fas/APO-1) death-inducing signaling complex. Cell 85, 817–827.
[2] Benoit, V., Chariot, A., Delacroix, L., Deregowski, V., Jacobs, N., Merville, M.P. and Bours, V. (2004) Caspase-8-dependent HER-2 cleavage in response to tumor necrosis factor alpha stimulation is counteracted by nuclear factor kappaB through c-FLIP-L expression. Cancer Res. 64, 2684–2691.
[3] Misra, R.S. et al. (2007) Caspase-8 and c-FLIPL associate in lipid rafts with NF-kappaB adaptors during T cell activation. J. Biol. Chem. 282, 19365–19374.
[4] Koenig, A., Russell, J.Q., Rodgers, W.A. and Budd, R.C. (2008) Spatial differences in active caspase-8 defines its role in T-cell activation versus cell death. Cell Death Differ. 15, 1701–1711.
[5] Sawasaki, T., Ogasawara, T., Morishita, R. and Endo, Y. (2002) A cell-free protein synthesis system for high-throughput proteomics. Proc. Natl. Acad. Sci. USA 99, 14652–14657.
[6] Sawasaki, T., Morishita, R., Gouda, M.D. and Endo, Y. (2007) Methods for high-throughput materialization of genetic information based on wheat germ cell-free expression system. Methods Mol. Biol. 375, 95–106.
[7] Goshima, N. et al. (2008) Human protein factory for converting the transcriptome into an in vitro-expressed proteome. Nat. Methods 5, 1011–1017.
[8] Tadokoro, D., Takahama, S., Shimizu, K., Hayashi, S., Endo, Y. and Sawasaki, T. (2010) Characterization of a caspase-3-substrate kinome using an N- and C-terminally tagged protein kinase library produced by a cell-free system. Cell Death Dis. 1, e89.
[9] Sawasaki, T., Kamura, N., Matsunaga, S., Saeki, M., Tsuchimochi, M., Morishita, R. and Endo, Y. (2008) Arabidopsis HY5 protein functions as a DNA-binding tag for purification and functional immobilization of proteins on agarose/DNA microplate. FEBS Lett. 582, 221–228.
[10] Sawasaki, T., Hasegawa, Y., Tsuchimochi, M., Kamura, N., Ogasawara, T., Kuroita, T. and Endo, Y. (2002) A bilayer cell-free protein synthesis system for high-throughput screening of gene products. FEBS Lett. 514, 102–105.
[11] Li, H., Zhu, H., Xu, C.J. and Yuan, J. (1998) Cleavage of BID by caspase 8 mediates the mitochondrial damage in the Fas pathway of apoptosis. Cell 94, 491–501.
[12] Medema, J.P., Scaffidi, C., Kischkel, F.C., Shevchenko, A., Mann, M., Krammer, P.H. and Peter, M.E. (1997) FLICE is activated by association with the CD95 death-inducing signaling complex (DISC). EMBO J. 16, 2794–2804.
[13] Ozaki, K., Kikly, K., Michalovich, D., Young, P.R. and Leonard, W.J. (2000) Cloning of a type I cytokine receptor most related to the IL-2 receptor beta chain. Proc. Natl. Acad. Sci. USA 97, 11439–11444.
[14] Asao, H., Okuyama, C., Kumaki, S., Ishii, N., Tsuchiya, S., Foster, D. and Sugamura, K. (2001) Cutting edge: the common gamma-chain is an indispensable subunit of the IL-21 receptor complex. J. Immunol. 167, 1–5.
[15] Jin, H., Carrio, R., Yu, A. and Malek, T.R. (2004) Distinct activation signals determine whether IL-21 induces B cell costimulation, growth arrest, or Bim-dependent apoptosis. J. Immunol. 173, 657–665.
[16] Juo, P., Kuo, C.J., Yuan, J. and Blenis, J. (1998) Essential requirement for caspase-8/FLICE in the initiation of the Fas-induced apoptotic cascade. Curr. Biol. 8, 1001–1008.
[17] Cerretti, D.P. et al. (1992) Molecular cloning of the interleukin-1 beta converting enzyme. Science 256, 97–100.
[18] Leonard, W.J. and Spolski, R. (2005) Interleukin-21: a modulator of lymphoid proliferation, apoptosis and differentiation. Nat. Rev. Immunol. 5, 688–698.
[19] Yi, C.H. and Yuan, J. (2009) The Jekyll and Hyde functions of caspases. Dev. Cell 16, 21–34.
[20] Akamatsu, N. et al. (2007) High IL-21 receptor expression and apoptosis induction by IL-21 in follicular lymphoma. Cancer Lett. 256, 196–206.
[21] de Totero, D. et al. (2006) Interleukin-21 receptor (IL-21R) is up-regulated by CD40 triggering and mediates proapoptotic signals in chronic lymphocytic leukemia B cells. Blood 107, 3708–3715.
[22] Brenne, A.T., Ro, T.B., Waage, A., Sundan, A., Borset, M. and Hjorth-Hansen, H. (2002) Interleukin-21 is a growth and survival factor for human myeloma cells. Blood 99, 3756–3762.

Phytochemistry 72 (2011) 1136–1144

Contents lists available at ScienceDirect

Phytochemistry

journal homepage: www.elsevier.com/locate/phytochem

Autophosphorylation profiling of Arabidopsis protein kinases using the cell-free system

Keiichirou Nemoto [a,b], Takuya Seto [a], Hirotaka Takahashi [a,b,c], Akira Nozawa [a,b], Motoaki Seki [d], Kazuo Shinozaki [e], Yaeta Endo [a,b,f,g,*], Tatsuya Sawasaki [a,b,f,g,*]

[a] Cell-Free Science and Technology Research Center, Ehime University, Matsuyama 790-8577, Japan
[b] The Venture Business Laboratory, Ehime University, Matsuyama 790-8577, Japan
[c] Department of Microbiology, Yong Loo Lin School of Medicine, National University of Singapore, Singapore 117597, Singapore
[d] Plant Functional Genomics Research Group, 1-7-22 Suehiro-cho, Tsurumi-ku, Yokohama, Kanagawa 230-0045, Japan
[e] Gene Discovery Research Group, RIKEN Plant Science Center, 1-7-22 Suehiro-cho, Tsurumi-ku, Yokohama, Kanagawa 230-0045, Japan
[f] Proteo-Medicine Research Center, Ehime University, Toon, Ehime 791-0295, Japan
[g] RIKEN Systems and Structural Biology Center, 1-7-22 Suehiro-cho, Tsurumi, Yokohama 230-0045, Japan

ARTICLE INFO

Article history:
Available online 7 April 2011

Keywords:
Wheat germ cell-free protein synthesis system
Arabidopsis cDNA library
Protein kinase
Autophosphorylation
Profiling

ABSTRACT

Protein phosphorylation is one of the main process in the signal transduction pathway. In recent years, there has been increasing attention to plant phosphorylation signaling and many laboratories are trying to elucidate pathways using various approaches. Although more than 1000 protein kinase (PK) genes have been annotated in the *Arabidopsis* genome, biochemical characterization of those PKs is limited. In this work, we demonstrate high-throughput profiling of serine/threonine autophosphorylation activity by a combination of the 759N-terminal biotinylated proteins library, produced using a wheat germ cell-free protein production system, and a commercially available luminescence system. Luminescent analysis revealed that 179 of the 759 PKs had autophosphorylation activity. From these 179 PKs, 67 of the most active PKs were analyzed to determine their function using the PlantP database. This analysis revealed that 35 (53%) of the proteins were classified as non-transmembrane protein kinases, and 15 (23%) were receptor-like protein kinases. Additionally, PKs from Group 4.4-MAP3K, Group 1.6, Group 4.5-MAPK/CDC/CK2/GSK kinases and Group 1.10-receptor like cytoplasmic kinases contained the highest percentage of autophosphorylated activity. Next, to get a better overview of the annotated 67 PKs, we used the gene ontology annotation search on the TAIR website to classify the 67 PKs into functional category. As a result, some of these PKs may be involved in phospho-signaling pathways such as signal transduction, stress response, and the regulation of cell division. Information from this study may shed light on many unknown plant PKs. This study will be a basis for understanding the function of PKs in phosphorylation network for future research.

1. Introduction

In metazoa, protein phosphorylation is a key function in signal transduction pathways for a wide range of processes including hormone response, inflammation, differentiation, development, and cancer formation. It has been shown that like metazoa, plants also utilize a phosphorylation signaling system. PKs are one of the largest gene families, representing ~4% (more than 1000) of all the genes in *Arabidopsis*. Plant PKs exhibit a high degree of duplication and there may be functional redundancy (Shiu and Bleecker, 2001), making a functional genomics approach for these proteins particularly relevant.

Autophosphorylation of PK is an important aspect of host regulation systems as these proteins are conformationally stabilized to maximize substrate recognition (Huse and Kuriyan, 2002). Ca^{2+}-dependent protein kinases (CPKs) act as sensors for intracellular Ca^{2+} fluxes and translate them into physiological responses by reversibly phosphorylating Ser/Thr residues of relevant essential enzymes (Roberts and Harmon, 1992). As an example of functional regulation by autophosphorylation, many of the reported CPKs has been shown to have autophosphorylation activity *in vitro* in the presence of Ca^{2+} (Harmon et al., 1987; Binder et al., 1994; Frylinck and Dubery, 1998; Yoon et al., 1999; Anil et al., 2000; Sawasaki et al., 2004; Hegeman et al., 2006). Autophosphorylation of CPK stringently reflects the intensity of the phosphorylation of substrate targets (Chaudhuri et al., 1999; Chehab et al., 2004). As

* Corresponding authors at: Cell-Free Science and Technology Research Center, Ehime University, Matsuyama 790-8577, Japan. Tel.: +81 89 927 9936; fax: +81 89 927 9941 (Y. Endo), tel.: +81 89 927 8530; fax: +81 89 927 9941 (T. Sawasaki).
E-mail addresses: yendo@eng.ehime-u.ac.jp (Y. Endo), sawasaki@eng.ehime-u.ac.jp (T. Sawasaki).

0031-9422/$ - see front matter Crown Copyright © 2011 Published by Elsevier Ltd. All rights reserved.
doi:10.1016/j.phytochem.2011.02.029

another example, autophosphorylation involves in brassinosteroids (BR) signaling pathway. The BR receptor-like kinase, BRI1, induces hetero-oligomerization of BRI1 and BAK1 and autophosphorylation of numerous Thr and Tyr residues to initiate BR signal transduction after BR binding (Nam and Li, 2002; Li et al., 2002; Wang et al., 2005; Oh et al., 2009). Another important PK in the BR signaling pathway that is activated by autophosphorylation is the GSK3/shaggy-like PK BIN2 (Kim et al., 2009). The active, phosphorylated, form of BIN2 phosphorylates the transcriptional factors BES1 and BZR which results in their degradation by the proteasome (He et al., 2002; Li and Nam 2002; Kim et al., 2009). Thus, the BIN2 is believed to negatively regulate the BR signaling pathway. These reports indicate that identifying the autophosphorylation activity of plant PKs are an important issue for understanding its regulation mechanism.

However, information about biochemical characterization of PKs has been hindered by the difficulties in obtaining sufficient quantities of functionally active recombinant protein. Conventional recombinant technologies utilizing cell-based protein production systems are well developed and to some extent can serve for both screening and expression. Nevertheless, they possess many intrinsic limitations. Primarily, cannot express proteins that induce cytotoxic effect in cells. Secondly, require time-consuming processes, such as sub-cloning, cell culture and protein purification. Finally, require high quality purification of PKs for functional screening because the host cell has high endogenous phosphorylation activities. Although current cell-free protein expression systems are known to synthesize proteins with high speed and accuracy, the yields of the products are low due to their instability over time. In addition to that, prokaryotic-based systems as represented by *Escherichia coli* cell-free systems are not always suitable for the expression of eukaryotic proteins because of the prokaryotic nature of its translation and folding mechanisms, that is, multidomain proteins found more often in eukaryotes than in prokaryotes, tend to missfold in prokaryotic systems, whether *in vivo* or *in vitro* (Netzer and Hartl, 1997).

A wheat germ cell-free protein production system could synthesize large numbers of proteins with high speed and accuracy, approaching those of *in vivo* translation, and could also express proteins which interfere with the host cell physiology (Kurland, 1982; Pavlov and Ehrenberg, 1996; Madin et al., 2000; Sawasaki et al., 2002a; Endo and Sawasaki, 2004). Using this system, we synthesized over 400 eukaryotic PKs (Sawasaki et al., 2004; Endo and Sawasaki, 2006; Tadokoro et al., 2010). These studies indicated that the wheat germ cell-free system had low endogenous phosphorylation activity. We recently generated a method to label monobiotin proteins that had been synthesized in the wheat cell-free system (Sawasaki et al., 2008). By combining this technology with a commercially available luminescence system, we also developed a high-throughput and high-sensitivity method for protein biochemical analysis. This method was able to specifically detect protease cleavage (Tadokoro et al., 2010), protein ubiquitination (Takahashi et al., 2009), protein–protein interaction (Ryo et al., 2008) and an autoantibody in the serum (Matsuoka et al., 2010), using unpurified (crude) recombinant protein. In this study, we applied this system to analyze *Arabidopsis* PK autophosphorylation activity (the scheme is shown Fig 1a and b).

2. Results

2.1. Autophosphorylation of biotinylated AtCPK3 and AtCPK13 were detected with high sensitivity and specificity using a luminescence system

We adapted the AlphaScreen technology for detecting interactions between autophosphorylated PKs and anti-phosphoserine/phosphothreonine (anti-pSer/pThr) antibody. This principle is illustrated in Fig. 1b. For autophosphorylation analysis of the expressed proteins, the translation mixture was used without any purification. In the AlphaScreen system, autophosphorylation of the biotinylated protein results in a biotinylated protein-anti-pSer/pThr antibody complex that is captured simultaneously by the streptavidin-coated donor beads, which is bound to the biotinylated PK, and the protein A-conjugated acceptor bead, which is bound to the anti-pSer/pThr antibody. The resultant proximity of the acceptor and donor bead generates the luminescent signal upon excitation at 680 nm.

To validate this system, we used the well-characterized calcium-dependent PKs AtCPK3 and AtCPK13 (Kanchiswamy et al., 2010). Biotinylated or non-biotinylated recombinant AtCPK3, AtCPK13 and dihydrofolate reductase (DHFR), serving as a negative control, were synthesized in the wheat germ cell-free system. As a

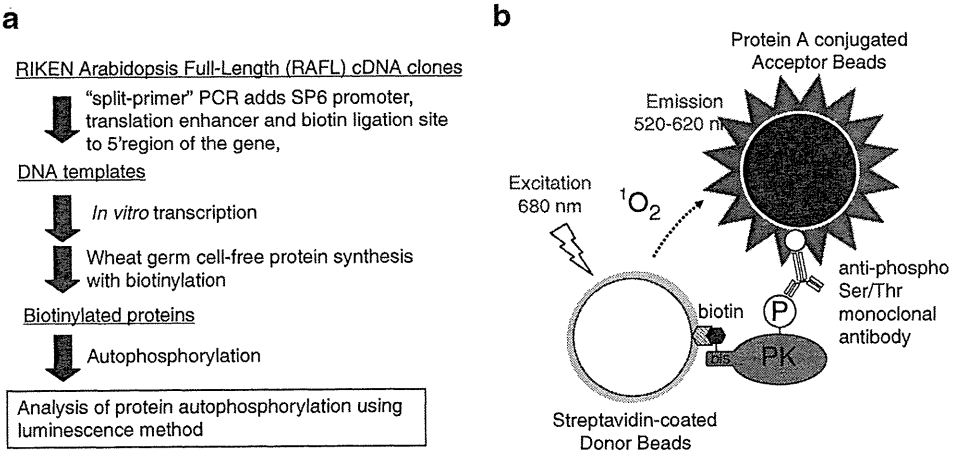

Fig. 1. Schematic diagram for determining autophosphorylation activity using a biotinylated PK library synthesized using the wheat germ cell-free system. (a) Flow chart of the cell-free expression procedures for high-throughput autophosphorylation profiling of *Arabidopsis* PKs. The method begins with generation of DNA templates generated by "Split-primer" PCR, followed by *in vitro* transcription using phage coded SP6 RNA polymerase, and finally translation in a bilayer reaction. All of the steps were carried out in 96-well microtiter plates. (b) Autophosphorylation analysis of the biotinylated PK using a luminescence system. Protein A-conjugated acceptor beads bound to anti-pSer/pThr monoclonal antibody and streptavidin-coated donor beads bound to biotinylated protein are in close proximity. Upon excitation at 680 nm, a singlet oxygen is generated by the donor beads, transferred to the acceptor beads within 200 nm, and the resultant reaction emits light at 520–620 nm.

result, a high luminescent signal was observed in the presence of biotinylated recombinant AtCPK3, and AtCPK13 (Fig 2a). In contrast, non-biotinylated PKs and DHFR showed very low signals. These luminescent signals were approximately consistent with autoradiography of *in vitro* kinase assay data (Kanchiswamy et al., 2010). These results indicate that the luminescent method can detect autophosphorylation by using an anti-pSer/pThr antibody.

2.2. Construction of a biotinylated protein kinase library using the wheat germ cell-free protein production system

To address high-throughput protein production, we have utilized our wheat germ high-throughput protein synthesis system (Madin et al., 2000; Sawasaki et al., 2002a), which can produce large numbers of recombinant proteins using a fully automated robot (Sawasaki et al., 2005). To create a library of *Arabidopsis* PKs, we selected 768 cDNAs encoding PKs from the RAFL cDNA resource. Since the full-length cDNA was provided in plasmids, the transcriptional template was synthesized by PCR directly from *E. coli* cells carrying cDNA clones, to avoid time-consuming cloning procedure. For biotinylation, a biotin ligation site (bls) was fused onto 5′ end of a target gene using the "split-primer" PCR method, and the reaction was started with *E. coli* cells (Sawasaki et al., 2002a). 759 (98.8%) out of 768 genes were successfully amplified and of those, 759 were transcribed. Protein production was performed automatically using the GenDecoder1000 protein synthesizer with standard 96-well microtiter plates (Sawasaki et al., 2007). After an 18 h incubation at 16 °C, randomly selected 30 proteins were confirmed by SDS–PAGE combined with immunoblot analysis using streptavidin Alexa Fluor 488 conjugate (Invitrogen, Carlsbad, CA) (data not shown). All 759 clones were produced as biotinylated proteins (Supplementary data 1).

2.3. High-throughput analysis for Ser/Thr autophosphorylation activity using a biotinylated protein kinase library

To identify autophosphorylation proteins that react with an anti-pSer/pThr antibody, biotinylated and non-biotinylated PKs libraries were prepared. In each well of a 384-well plate, a translation mixture expressing biotinylated or non-biotinylated PK was incubated for 60 min, and subsequently a mixture of donor and acceptor beads and anti-pSer/pThr antibody were added to each well. After incubation, autophosphorylation of the biotinylated PK was detected by the luminescence assay shown on Fig. 1b. All data are the average of two independent experiments, and the background was controlled for each using the relevant non-biotinylated PK. Fig. 2b graphs the relative luminescent signals (biotinylated PK/non-biotinylated PK) of each PK. As a result, 179 out of 759 PKs demonstrated a relative luminescent signal higher than 5-fold. This assay also showed 67 PKs having a relative luminescence signal higher than 10-fold (Fig 3a). Two of these 67, AtMPK17 (at2g01450) and AtCPK6 (at2g17290) exhibited around 100 relative luminescence signals (Fig 3a). We compared our results with autophosphorylation data from a previous *in vitro* study monitored by autoradiography (Supplementary data 1; Sawasaki et al., 2004a). Of the 179 PKs that demonstrated autophosphorylation in this work, 125 were tested previously. Of these 125 PKs, 81 (64.8%) had autophosphorylation activity in the previous study. Since more than half of 179 PKs had autophosphorylation activity, that a relative luminescence signal higher than 5-fold was defined as autophosphorylation activity. Additionally, 55 out of the high relative luminescence signal ($\geqslant$10-fold) 67 PKs has been analyzed in the previous study, and 45PKs (81.8%) had autophosphorylation activity.

In general, when around 700 PKs are analyzed by autoradiography, it takes at least 2 weeks. In contrast, this method is able to analyze in only 3 h. Therefore, this method is a powerful tool for high-throughput protein phosphorylation analysis.

2.4. Functional classification analysis of high autophosphorylation protein kinases

We next classify high relative luminescence signal 67 PKs according to both their primary sequence and functions. With the completion of the *Arabidopsis* genome sequencing, a classification of the PKs has been reported and the database is available at PlantP (http://www.plantsp.sdsc.edu/) (Gribskov et al., 2001). Using this database, functional classification of the 67 PKs noted above was analyzed. According to PlantP classification, the largest class of the 67 PKs was non-transmembrane protein kinases [Class IV, 53% (35 PKs)] (Fig. 3b). PKs in this class do not have an identifiable transmembrane domain (TMD), indicating that are not closely related to the transmembrane receptor kinases. Class IV PKs play a central role in the transduction of various extra- and intracellular signals (e.g. MAPK, calcium response kinase). The next class was receptor-like protein kinases (RLK) [Class 1, 23% (13 Pks)]. RLKs are defined by the presence of a signal peptide, an extracellular domain, a TMD and a C-terminal Ser/Thr kinase domain (Shiu and Bleecker, 2001), which are involved in symbiosis (Parniske 2008), disease resistance (Afzal et al., 2008), self-incompatibility (Takayama and Isogai, 2005), BR signaling

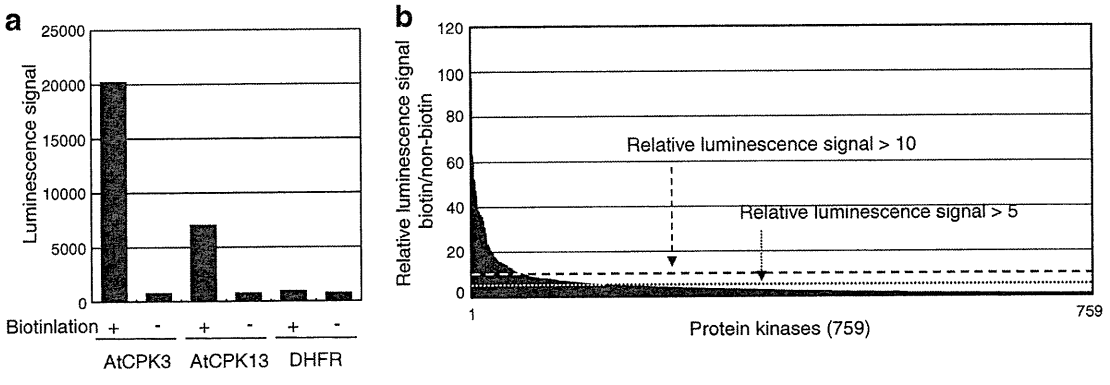

Fig. 2. High-throughput production and autophosphorylation activity profiling of *Arabidopsis* PKs. (a) Autophosphorylation of biotinylated AtCPK3 and AtCPK13 were detected by the luminescence system. (b) Autophosphorylation of 759 biotinylated PKs synthesized using the wheat germ cell-free system, as described in the text, were detected by the luminescence system. All data are the average of two independent experiments, and the background was controlled for each using the relevant non-biotinylated PK.

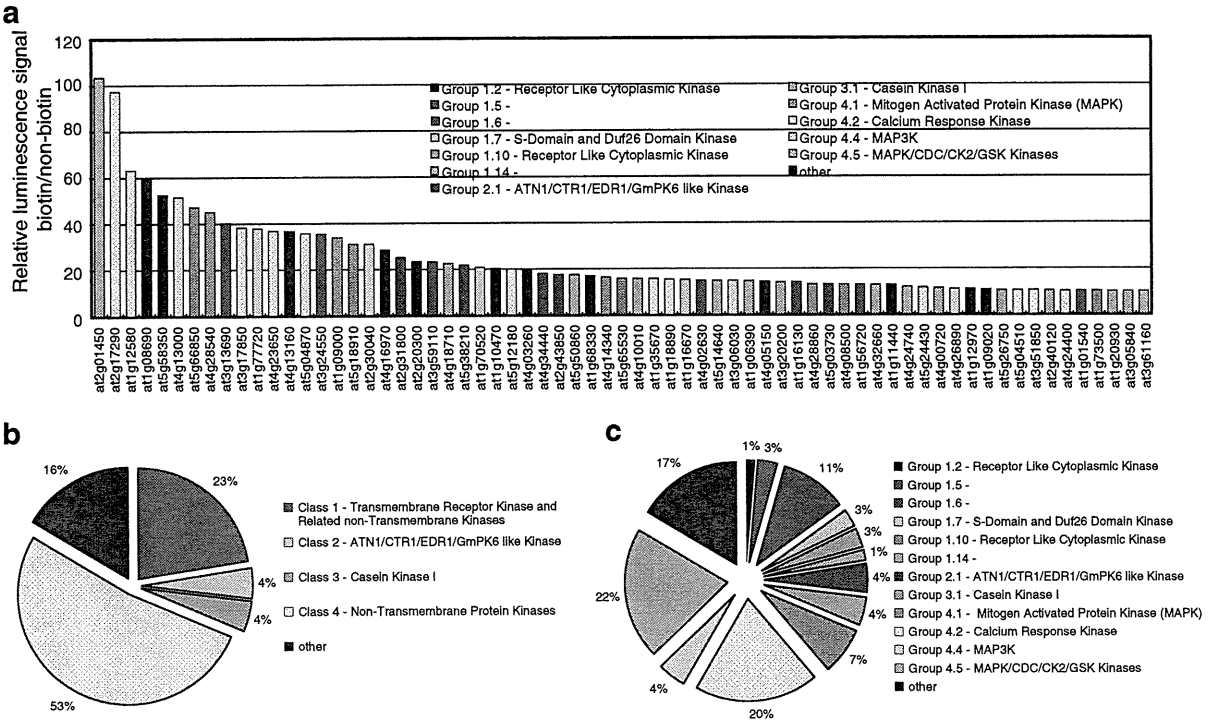

Fig. 3. Functional distribution of 67 high luminescent signal PKs. (a) Sixty-seven highly signal biotinylated PKs were selected based on luminescent signal ⩾10-fold background signal. This data is average of two independent experiments, and the background control for each was the relevant non-biotinylated PK. (b and c) The 67 PKs were grouped by the corresponding PlantP database classification number and classified by (b) Class and (c) Group.

(Belkhadir and Chory, 2006), cell growth regulation (Hematy and Hofte, 2008) and formation of the shoot stem cell niche (Clark, 2001; Stahl and Simon, 2005).

We next annotated the 67 PKs by PK Groups using the PlantP database. Interestingly, the groups represented included MAPK/CDC/CK2/GSK kinases [Group 4.5, (22%)], calcium response kinases [Group 4.2 (20%)], unclassified protein kinases (17%) and Group 1.6 (11%) (Fig 3c). Additionally, MAP3 K [Group 4.4, (50%)], Group 1.6 (35%), MAPK/CDC/CK2/GSK kinases [Group 4.5, (23%)] and receptor like cytoplasmic kinase [Group 1.10 (22%)] had the highest percentage of autophosphorylating PKs (Fig. 4).

Finally, to get a better overview of the annotated 67 PKs, we used the gene ontology annotation search on the TAIR website (Berardini et al., 2004) and classified the 67 PKs into functional category (Supplementary data 2 and Fig. 5). As a result, 19 out of 67 PKs were annotated in localization of plasma membrane, and those more than halves were classified into Groups 1.6 and 4.2. (Supplementary data 2). Moreover, the annotated proteins were involved in diverse biological functions such as hormone biosynthesis and response (6%), response to other stresses (5%), development (4%), response to abiotic or biotic stimulus (3%), signal transduction (3%), biological process unknown (2%), transport (1%), transcription (0.5%), cell organization and biogenesis (0.5%) (Fig. 5b).

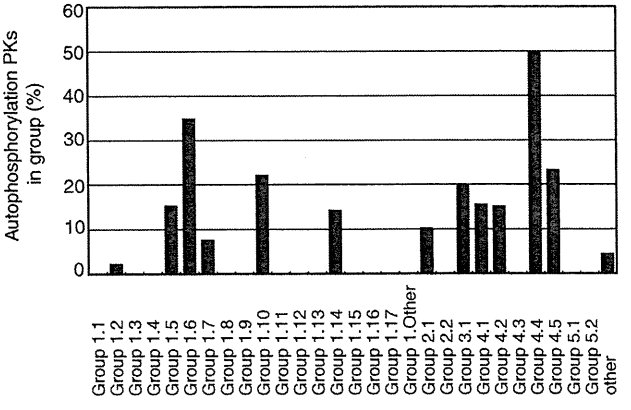

Fig. 4. PK groups compared by the percentage of protein autophosphorylation. Group 1.2; receptor like cytoplasmic kinase, Group 1.4; crinkly 4 like kinase, Group 1.7; S-domain and Duf26 domain kinase, Group 1.8; leucine rich repeat receptor kinase, Group 1.10; receptor like cytoplasmic kinase, Group 1.11; legume lectin domain kinase, Group 1.12; leucine rich repeat receptor kinase, Group 1.13; leucine rich repeat receptor kinase, Group 1.16; receptor like cytoplasmic kinase, Group 1.17; wall associated kinase, Group 2.1; ATN1/CTR1/EDR1/GmPK6 like kinase, Group 2.2; unknown function protein kinase, Group 3.1; casein kinase I, Group 4.1; mitogen activated protein kinase, Group 4.2; calcium response kinase, Group 4.3; unknown function protein kinase, Group 4.4; MAP3 K, Group 4.5; MAPK/CDC/CK2/GSK kinases, Group 5.1; other protein kinase, Group 5.2; other protein kinase, other; unclassified PKs (group unnamed). The classification numbers correspond to the PlantP database.

3. Discussion

Phosphorylation of protein is an important property of protein regulations reported both from the plants as well as animals. Autophosphorylation may also be important not only as a modulator of PK activity (Chehab et al., 2004) but also as a means of altering protein binding properties that can affect a broad range of functional properties from cellular localization (Nayler et al., 1998.) to substrate interactions (Fan et al., 2004.) to macromolecular complex formation (Ikeda et al., 2000; Merkle et al., 2002). Therefore, analysis of the autophosphorylation activity of plant PKs is a key issue for understanding its regulation mechanism. The plant PKs functions have been revealed by primarily genetic approaches such as loss and gain of gene function in plant. Moreover, recent studies

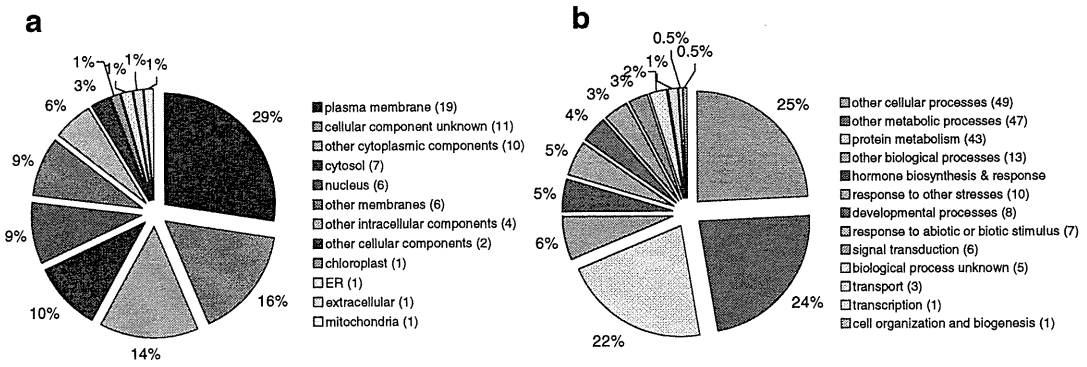

Fig. 5. Gene ontology classification of 67 high luminescent signal PKs. The 67 high luminescent signal PKs were grouped by (a) cellular Component and (b) biological process based on Arabidopsis gene ontology annotation. Gene counts and percentages are listed for each category. Because a single gene may have more than one functional annotation, the gene counts do not add up to the total number of analyzed genes. Numbers in parentheses indicate the number of genes in each annotation group.

found many of phosphopeptides in *Arabidopsis* by MS-based phosphoproteomic screens (Benschop et al., 2007; de la Fuente van Bentem et al., 2008; Sugiyama et al., 2008). However, information about biochemical characterization of PKs has been limited.

To solve this problem, we developed a simple and highly sensitive autophosphorylation analysis method by combination of the wheat germ cell-free protein synthesis system and luminescent detection system (Fig. 1a and b). One advantage of this method is that the wheat germ cell-free protein synthesis system can produce large numbers of quantity and good quality recombinant proteins without time-consuming cloning and protein purification steps (Madin et al., 2000; Sawasaki et al., 2002a, 2005.). In addition, there is no extreme difference in the concentration of the synthesized protein (Nozawa et al., 2009). Second, the luminescence system that combines the biotinylated proteins is able to specifically detect protein modification (Takahashi et al., 2009; Tadokoro et al., 2010) and protein–protein interactions (Ryo et al., 2008; Matsuoka et al., 2010). Using this method, we conveniently detected autophosphorylation of biotinylated AtCPK3 and AtCPK13 (Fig. 2a). Thus, this method represents a simple and quick alternative to conventional laborious kinase assays using [γ-^{32}P]-ATP.

We synthesized the 759 biotinylated PKs of *Arabidopsis* and applied for the autophosphorylation assay (Fig. 2b, Supplementary data 1). As a result, we identified 179 PKs having a relative luminescence signal than 5-fold. Comparing to the previous study, 179 PKs are expected to have the autophosphorylation activity. This assay also showed 67PKs of high relative luminescence signal (Fig. 3a and Table 1). It is thought that 67 PKs has the high autophosphorylation activity when based on the principle of the antibody detection that the signal value is correlation to the number of phosphorylated peptide. However, the three-dimensional conformation effects of PK against the accessibility and specificity of the antibodies cannot be discounted. Unfortunately, currently available antibodies against phospho-Ser/Thr residues generally may have low affinity and be specific to the surrounding amino acid sequence. Therefore, the anti-pSer/pThr antibody of the independent to the surrounding amino acid sequence should be developed to improve this assay system.

Using PlantP database, functional classification of the 67 PKs was analyzed. Interestingly, non-transmembrane protein kinases [Class IV] accounted for half of the 67 PKs, and MAPK/CDC/CK2/GSK kinases [Group 4.5] and calcium response kinases [Group 4.2] were the most of it (Fig. 3a and b). Besides, MAP3K [Group 4.4, (50%)], Group 1.6 (35%) had the highest percentage of autophosphorylating PKs (Fig. 4). MAP3K involved in the activation of the MAP kinase cascade. This result has been suggested that MAP3K phosphorylation activity is enhanced by autophosphorylation, as is proposed for other eukaryotes MAP3Ks (Nishihama et al., 2002). However, the autophosphorylation activity of other MPKs except AtMPK17 are not admitted. In mammals, MPKs show some Tyr kinase activity and may autophosphorylate on both Thr and Tyr residues (Wu et al., 1991). The autophosphorylation may increase the affinity of MAP2K for MPK (Haystead et al., 1992). In our studies, plant MPKs exhibit little autophosphorylation activity, therefore functional regulation by autophosphorylation might be different from mammals (Roux and Blenis, 2004; Pimienta and Pascual, 2007).

In our studies, the seven of GSK3/Shaggy like PKs showed a high autophosphorylation activity, and other 3 PKs had autophosphorylation activitiy (Supplementary data 1). GSK3/Shaggy like PKs were isolated from *Arabidopsis* as Shaggy (in *Drosophila melanogaster*) and GSK-3 (in mammals) homologues gene (Bianchi et al., 1994; Jonak et al., 1995). Mammalian GSK-3 expressed in bacteria shows evidence of autophosphorylation on Tyr, Ser/Thr residues, which raises the possibility, that Tyr phosphorylation of GSK-3 in mammalian cells is an autocatalytic event (Wang et al., 1994.). As well as GSK-3, BIN2 activity is controlled by autophosphorylation of Tyr residues in T-loop (Kim et al., 2009). However, the functional role of autophosphorylation of Ser/Thr residues is unclear. In mammals, the role of cis/trans-phosphorylation (itself or other kinase) of Ser/Thr residues has been suggested to cause inactivation of enzyme (Wang et al., 1994; Cross et al., 1995). In plants, it might influence the activity and complex formation, localization of GSK/shaggy PKs by autophosphorylation of Ser/Thr residues.

The 19 out of 67 PKs were annotated with localization of plasma membrane, and those more than halves were classified into Groups 1.6 and 4.2. (Table 1). Furthermore, many of Calcium response kinases [Group 4.2] (including of CPKs) were annotated with involved in ABA mediated signaling (Supplementary data 2). Many of the reported CPKs have shown autophosphorylation activity *in vitro* in the presence of Ca^{2+} (Harmon et al., 1987; Binder et al., 1994; Frylinck and Dubery, 1998; Yoon et al., 1999; Anil et al., 2000; Hegeman et al., 2006). Many stress signals, such as wounding, cold, high salinity, and drought, are known to elicit fluctuations in cytosolic Ca^{2+} levels, as well as changes in protein phosphorylation (Bush, 1995; Trewavas, 1999; Knight and Knight, 2001). Several lines of evidence suggest that CPKs mediate abiotic stress signaling pathways (Urao et al., 1994; Monroy and Dhindsa, 1995; Botella et al., 1996; Yoon et al., 1999; Patharkar and Cushman, 2000; Saijo et al., 2000; Chico et al., 2002; Xu et al., 2010). On the other hand, the best-studied *A. thaliana* PERK [Group 1.6], PERK4 is a positive regulator implicated in the early stage of ABA signaling, which modulates root cell elongation, and its effects are mediated by Ca^{2+} (Bai et al., 2009). In the presence of ABA, PERK4 is activated though autophosphorylation, which leads to activation of Ca^{2+} channel and stimulation expression of genes

Table 1
Summary of autophosphorylation activity of 67 Arabidopsis protein kinases.

No. of Arabidopsis genes	PlantP funciton[a]	PlantP symbol[a]	PlantP no.[a]	PlantP family[a]	Relative luminescence signal[b]	Autophosphorylation[c]
at2g01450	Putative mitogen activated protein kinase 17	AtMPK17	21188	Family 4.5.1 – MAPK family	103.5	Yes
at2g17290	Calcium-dependent protein kinase, isoform 6	CPK06	26192	Family 4.2.1 – calcium dependent protein kinase	97.3	Yes
at1g12580	Phosphoenolpyruvate carboxylase-related kinase	PEPRK1	21496	Family 4.2.1 – calcium dependent protein kinase	63.2	Yes
at1g08690	–	–	–	–	60.1	–
at5g58350	WNK kinase 4	–	37670	–	52.4	–
at4g13000	Putative protein kinase	–	21830	Family 4.2.6 – IRE/NPH/PI dependent/S6 kinase	51.4	Yes
at5g66850	Putative MAP3 K	–	22064	Family 4.1.1 – MAP3 K	47.3	Yes
at4g28540	Putative casein kinase 1	–	21883	Family 3.1.1 – Casein kinase I family	45.1	Yes
at3g13690	Putative protein kinase	–	21717	Family 1.6.2 – Plant external response like kinase	40.3	Yes
at3g17850	Putative protein kinase	–	21210	Family 4.2.6 – IRE/NPH/PI dependent/S6 kinase	38.3	Yes
at1g77720	Putative homolog to msp1 protein kinase	–	21464	Family 4.4.4 – Unknown function kinase	37.8	Yes
at4g23650	Calcium-dependent protein kinase, isoform 3	CPK03	21867	Family 4.2.1 – Calcium dependent protein kinase	36.8	Yes
at4g13160	–	–	–	–	36.6	–
at5g04870	Calcium-dependent protein kinase, isoform 1	CPK01	21951	Family 4.2.1 – Calcium dependent protein kinase	35.7	Yes
at3g24550	Protein kinase	–	21699	Family 1.6.2 – Plant external response like kinase	35.5	Yes
at1g09000	Putative NPK1-related protein kinase 2	–	21067	Family 4.1.1 – MAP3 K	33.9	Yes
at5g18910	Pto kinase interactor 1	–	21302	Family 1.10.1 – Receptor like cytoplasmic kinase VI	31.0	Yes
at2g30040	Putative protein kinase	–	21643	Family 4.4.1 – Unknown function kinase	31.0	nd
at4g16970	Putative casein kinase II	–	21930	-	28.4	–
at2g31800	Putative protein kinase	–	21523	Family 2.1.2 – Ankyrin repeat domain kinase	25.2	nd
at2g20300	Putative protein kinase	–	21557	Family 1.2.2 – Receptor like cytoplasmic kinase VII	23.4	Yes
at3g59110	Receptor like protein kinase	–	21782	Family 1.6.3 – Receptor like cytoplasmic kinase V	23.2	Yes
at4g18710	GSK3/shaggy-like protein kinase eta	ASK-eta	21835	Family 4.5.4 – GSK3/shaggy like protein kinase family	22.6	Yes
at5g38210	Wall-associated kinase	–	21317	Family 1.5.2 – LRK10 like kinase (Type 1)	21.9	Yes
at1g70520	Putative protein kinase	–	21455	Family 1.7.2 – Domain of unknown function 26 (DUF26) kinase	20.8	Yes
at1g10470	Cytokinin-induced response regulator protein	–	32297	-	20.3	–
at5g12180	Calcium-dependent Protein Kinase, isoform 17	CPK17	21973	Family 4.2.1 – Calcium dependent protein kinase	20.0	Yes
at4g03260	Protein phosphatase regulatory subunit	–	10885	-	19.5	–
at4g34440	Putative ser/thr protein kinase	–	21909	Family 1.6.2 – plant external response like kinase	18.1	Yes
at2g43850	Putative protein kinase	–	21516	Family 2.1.2 – ankyrin repeat domain kinase	17.6	Yes
at5g50860	Cyclin-dependent protein kinase like	–	22022	Family 4.5.2 – CDC2 like kinase family	17.5	Yes
at1g68330	–	–	-	-	17.0	–
at4g14340	Putative casein kinase I	–	21925	Family 3.1.1 – casein kinase i family	16.4	Yes
at5g65530	Putative protein	–	22057	Family 1.10.1 – receptor like cytoplasmic kinase VI	15.8	nd
at4g10010	Putative protein kinase	–	21817	Family 4.5.2 – CDC2 like kinase family	15.7	–
at1g35670	Calcium-dependent Protein Kinase, isoform 11	CPK11	20998	Family 4.2.1 – calcium dependent protein kinase	15.7	Yes
at1g18890	Calcium-dependent Protein Kinase, isoform 10	CPK10	21443	Family 4.2.1 – calcium dependent protein kinase	15.5	Yes
at1g16670	Hypothetical protein	–	21169	Family 1.7.1 – S domain kinase (Type 1)	15.3	nd
at4g02630	Putative ser/thr protein kinase	–	21799	Family 1.6.3 – receptor like cytoplasmic kinase V	15.0	Yes
at5g14640	GSK3/shaggy-like protein kinase	–	21976	Family 4.5.4 – GSK3/shaggy like protein kinase family	14.8	Yes
at3g06030	NPK1-related protein kinase 3	–	21692	Family 4.1.1 – MAP3K	14.8	Yes
at1g06390	GSK3/shaggy-like protein kinase iota	ASK-iota	21488	Family 4.5.4 – GSK3/shaggy like protein kinase family	14.7	Yes
at4g05150	–	–	–	–	14.5	–
at3g20200	Putative protein kinase	–	21229	Family 1.14.2 – receptor like cytoplasmic kinase IX	14.1	nd
at1g16130	Similarity to wall-associated protein kinase 1	–	21088	Family 1.5.1 – wall associated kinase-like kinase	14.1	nd
at4g28860	Putative casein kinase I	–	21886	Family 3.1.1 – casein kinase I family	13.2	Yes
at5g03730	Protein kinase CTR1	CTR1	21949	Family 2.1.3 – CTR1/EDR1 kinase	13.2	Yes
at4g08500	Putative MAP3K	–	21814	Family 4.1.1 – MAP3K	13.1	nd
at1g56720	Putative protein kinase	–	21010	Family 1.6.3 – receptor like cytoplasmic kinase V	13.0	Yes
at4g32660	Protein kinase AME3	–	21902	Family 4.5.6 – LAMMER kinase family	12.9	Yes
at1g11440	–	–	–	–	12.9	–
at4g24740	Protein kinase	–	21871	Family 4.5.6 – LAMMER kinase family	12.1	Yes

(continued on next page)